

Bachelor Thesis

DEVELOPMENT OF A LUMINOPHORE DISPENSING MECHANISM TO BE USED IN THE DEEP SEA WITH THE FLUORESCENT SEDIMENT PROFILE IMAGING CAMERA

Author: Anneke Neber

Matr.Nr: 37386

April 26, 2023



First examiner: Prof. Dr. Axel Bochert

Second examiner: Dipl.-Ing. Normen Lochthofen

Acknowledgements

Herewith I want to thank everybody that supported me during my Bachelor studies, during my internship at AWI and during my bachelor's thesis.

Especially I want to thank Normen Lochthofen, who supported me with ideas, experience, and skills to develop my bachelor project. I also want to thank Janine Ludszuweit for her support with the manufacturing and guidance during the practical parts.

A big thanks to Axel Bochert, who oversaw my thesis. Also, I want to thank everybody who read the thesis and gave me feedback: Theresa Beer, Marita Quitzau, and Liza Maak. Also, I would like to thank my parents for supporting me throughout my whole studies.

Declaration of an oath

I hereby declare under oath that I have written this bachelor's thesis independently and without the help of others. All passages of the thesis, which are taken in the wording or the sense of publications or lectures of other authors, I have marked as such. The thesis has not been submitted, either in part or in its entirety, to any other examination authority or any other department of the Bremerhaven University of Applied Sciences.

April 26, 2023, Bremerhaven

Date, place

Signature

Abstract

For this study, it was planned to observe bioturbation with tracers which get dispensed in front of the Sediment Profile Imaging Camera (SPI). A device is needed for the dispensing of the luminophores. That is why, the Luminophore Dispensing Mechanism (LDM) was developed in this bachelor thesis. The used material such as the luminophores and the SPI will be explained. Also, the sinking behavior is observed. The expected sinking velocity as well as the lateral drift, due to currents near the seafloor, are calculated. For the development of the LDM, some pilot tests were executed to find the right method. It was decided to continue the idea of two movable grids, which can be aligned either for the apertures to be on top of each other or to be replaced so that nothing can be dispensed. The most important part is the development of the final design and the trigger. The trigger is crucial for the transition between the luminophore-containing and luminophore-emitting states.

The finished mechanism was tested both in a laboratory environment as well as in the North Sea during an expedition. Even though the LDM worked fine in the laboratory, problems did occur during the North Sea test as to the result of no useful image being taken by the SPI. Possibilities for improvements are given, while the basic idea can be continued for further studies.

List of Figures

1.1	Pictures taken with the SPI Camera by M. Solan [4] observing the behavior of a spider crab with visible luminophores, pink in color	1
2.1	Picture of the luminophores under the microscope, optical enlargement 1:100	4
2.2	Example of a picture taken with the SPI Camera in the German Bay during HE528 with the <i>RV Heincke</i> at the long term station H1 by Jennifer Dannheim	5
3.1	Lateral current depending on the distance of the luminophores to the seafloor	9
4.1	Preliminary test, method 1: Two movable grids, Inventor Sketch	12
4.2	Preliminary test, method 2: Grid with movable hopper, Inventor Sketch . .	13
4.3	Comparing the two methods after the preliminary tests, pink luminophores were dispensed out of the prototypes (seen in orange)	14
5.1	Finished LDM, view of the mechanism from above, Inventor model	18
5.2	Finished LDM, view from the bottom, Inventor model	19
5.3	Upper Grid, view from above	20
5.4	View of the mounting, Inventor model	21
5.5	View of the activator, Inventor model	22
6.1	Product range of galvanic time release, the upper row shows releasing time ranging from 1 day to 14 days, the lower row shows costume releases ranging from one hour to 100 days [20]	24
6.2	Methods to apply pressure to the LDM with lever systems	25
6.3	Ideas with elastic springs	26
6.4	Manufactured LDM, fasten the elastic rope (the red rope), and with the activator (on the right) and the trigger, equipped with all springs and screws and one spout component	28
7.1	The LDM during the test in the aquarium	31
7.2	Sketch of the SPI Camera, drawn in Inventor	32
7.3	The LDM mounted in front of the SPI, on board of the <i>RV Heincke</i> , ready to be used	33
7.4	Lowering the SPI into the water from the <i>RV Heincke</i>	35
7.5	The LDM during the cruise with the <i>RV Heincke</i> after the fourth test . . .	35

Contents

List of figures	iv
1 Introduction	1
2 Theory	3
2.1 Experiments regarding bioturbation with luminophores	3
2.2 Luminophores	4
2.3 Luminescence	5
2.4 Type of result produced by the SPI	5
3 Sinking behavior of the luminophores	7
3.1 Lateral drift and current	8
4 Preliminary tests for different dispensing mechanisms	11
4.1 Planning	11
4.2 Criteria	11
4.3 Ideas for the mechanism	12
4.3.1 Two movable grids	12
4.3.2 Grid with movable hopper	13
4.4 Implementation	13
4.5 Evaluation	14
5 Basic design	17
5.1 Material and manufacturing	17
5.1.1 Manufacturing	17
5.1.2 Material	17
5.2 Mechanism	18
5.3 Mounting	21
5.4 Activator	21
5.4.1 Basis from the literature	22
5.4.2 Activator explained	22
6 Trigger	23
6.1 Type of Trigger	23
6.2 Criteria	24
6.3 Ideas	25
6.3.1 Pressure application through levers	25
6.3.2 Pressure application through springs	25
6.4 Decision	26
6.5 Dimensioning the spring force	28
6.5.1 Elastic force calculation for the springs	28
6.5.2 Friction coefficient calculation	29

7	Results	30
7.1	Implementing the LDM	30
7.2	Results from the tests in a laboratory environment	31
7.3	Experimental setup of the tests in the North Sea	31
7.4	Results from the tests in the North Sea	34
8	Discussion of the results	36
9	Conclusion	38
10	Bibliography	39
A	Technical drawings	iv
B	Data sheets and other	xii

1. Introduction

Climate change is rapidly altering the conditions of the environment. Particularly sensitive ecosystems are affected, such as the slow benthos of the Arctic deep sea. [1]

Therefore it is of utmost importance to investigate the conditions of this alteration and how it is already affecting the organisms of the deep sea. Due to the melting of the ice, which leads to major habitat changes, the Arctic is one of the fastest-changing places worldwide. Since the region is hard to access, the available data on bioturbation rates in the Arctic deep sea are scarce. [2]

Bioturbation is a very important soil phenomenon on land and in water, as it ensures the availability of oxygen in deeper sediment layers. It can be defined as the alteration of the existing structure in the sediment through animals.

Many organisms use the sediment to protect from predators or strong currents, to catch prey, or nurture their offspring. Digging through the sediment they leave burrows or other traces. Every organism living in or on the seafloor is impacted by the resulting bioturbation, as it causes changes in the surface and an influx of limited substances such as metabolites or oxygen. [3]

In the deep sea, bioturbation is especially important, as available oxygen is scarce. Also, the entire ecosystem depends on nutrients that are recycled from the organic matter deposited by the organisms. [2]

In order to gain data on bioturbation in the Arctic deep sea, a project was planned by Alfred-Wegener-Institute for polar research (AWI) to be executed in 2024. The method for this experiment includes placing luminophores in front of the Sediment Profile Imaging Camera (SPI) and observing the distribution caused by the organisms.

Various experiments use luminophores to track the movements of organism causing bioturbation. Typically, luminophores are placed with SCUBA divers in shallow water, or with a Remotely Operated Vehicle (ROV) in deeper water. Another approach is to bring the relevant soil to the surface and into aquariums, to then observe the bioturbation with luminophores. An example of taken results with luminophores dispensed on the seafloor can be seen in figure 1.1. [f-SPI] [2] [1]

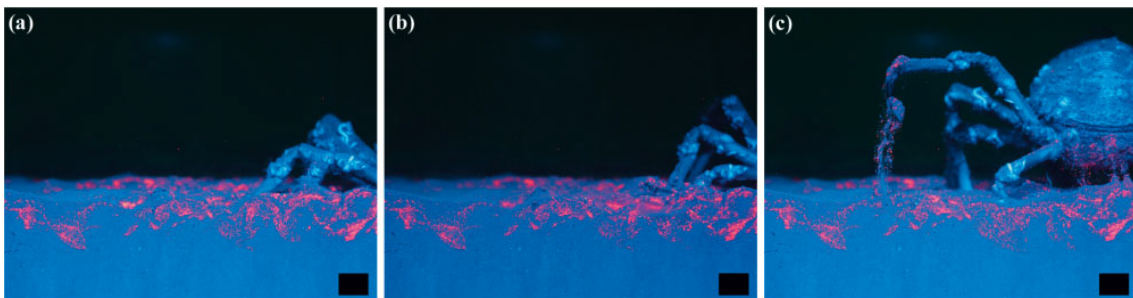


Figure 1.1: Pictures taken with the SPI Camera by M. Solan [4] observing the behavior of a spider crab with visible luminophores, pink in color

The main problem of this method until now is the expenditure that is necessary to dispense the luminophores. Both in situ methods, ROV and SCUBA diver, are neither cost nor time efficient, whilst additionally, SCUBA divers cannot operate in great depth.

Since all of these methods involve direct human input, errors might occur and the repeatability decreases.

As a solution, the Luminophore Dispensing Mechanism (LDM) was developed. It is planned to operate in great depth and dispenses the luminophores automatically leading to a shorter execution time without human input. Also, it is very cost-efficient and dispenses the tracers evenly over a determined area, making the experiment repeatable.

In the following bachelor thesis, the Luminophore Dispensing Mechanism is presented. Used material and previous experiments regarding bioturbation will be reviewed in chapter 2. Currents that might occur and other factors regarding the spread pattern are estimated in chapter 3. An approach through preliminary tests is discussed in chapter 4. Finishing the design for the mechanism and introducing the trigger is explained in chapter 5 and 6. Practical tests were conducted. The results can be seen in chapter 7, and are discussed in chapter 8. Lastly, chapter 9 gives a conclusion.

2. Theory

Bioturbation is crucial for the benthic ecosystem. Due to current developments such as climate change, it is important to be able to predict how an ecosystem will respond to changes. The deep sea is a low-energy environment where the distribution of nutrients depends solely on bioturbation. It is therefore important for science to gather more information about deep-sea bioturbation. [2]

Different organisms can be responsible for bioturbation, such as the spider crab in figure 1.1. However, mostly organisms that dig deeper into the soil are crucial for bioturbation. In the North Sea that can be, for instance, mussels, worms, and bigger animals such as mud lobsters (all of them were observed during the HE616 cruise, where the practical test for the LDM took place). The deep sea is the habitat of different benthic organisms, including animals from the invertebrate communities and the nematode communities. [1], [5]

2.1 Experiments regarding bioturbation with luminophores

The planned project for 2024 is based on similar experiments regarding luminophores and bioturbation.

To determine bioturbation, often luminophores are used. They are a reliable indicator of how much sediments from the surface get mixed into the soil. Depending on the study site, luminophores can be dispensed with SCUBA divers in shallow waters, or with a ROV in deeper waters. A usual method is the sampling with sample corers, to dry and slice the sediment into sections where each section represents a certain depth into the seafloor. Once the sample is dried, the luminophores can be counted. Through this method, an insight of the mixing rate is given. [2]

For better results, time series can be generated, which shows the mixing rates over time. A different possibility to do so is the lifting of the sediment to the surface. That way, the bioturbation can be observed in real time. [1]

A different method is using the SPI as fluorescent Sediment Profile Imaging (f-SPI). The SPI generally takes momentary images of the sediment layers of the seafloor. Through the use of an f-SPI, the flash is used with a filter, in order to stimulate the fluorescence of the luminophores.

A good example is the experiment that was conducted by M. Solan in 2003, at 28 m depth in the Gullmarsfjord in Sweden, where the SPI was used as f-SPI. The luminophores were spread by SCUBA divers in front of the camera. A photo was taken every ten minutes for a total of 16 hours. An example of a result could be seen in figure 1.1 in the introduction. The use of the f-SPI to generate a time series allows species to be determined. [4]

However, for a more regular use of the f-SPI, a more effective method has to be found to place luminophores. Different application methods were seen: with SCUBA divers, with a ROV, or by lifting the sediment to the surface. Problematic when using an ROV (or SCUBA divers) to dispense luminophores is the amount of time required to operate the vehicles and the cost of purchasing the ROV (or professional divers).

Moreover, in the deep sea, SCUBA divers cannot operate. Nor is lifting the sediment to

the surface a solution, as deep sea organisms could die in the atmospheric pressure. ROVs can manage great depth, though, if a SPI is used to collect data, it might be difficult with displacing the luminophores at a close distance to the glass window without bumping into the rack or even damaging the SPI.

For an implementation of the f-SPI experiments in the deep sea, an alternative solution must be found. The LDM was developed exactly for this application. The development of a device is an engineering problem. The challenges include automatic triggering, uniform distribution, and an application area with high pressure, low temperature, and high corrosion potential.

2.2 Luminophores

Luminophores play a critical role in this project. Luminophores are sediment-sized tracers, that can be optically distinguished from regular sediment. This allows the luminophores to blend with the sediment on the seafloor while simultaneously tracking their movement. [6]

In figure 2.1 the used luminophores are presented. This image was taken with a microscope to give an impression of the luminophores' size and outline.

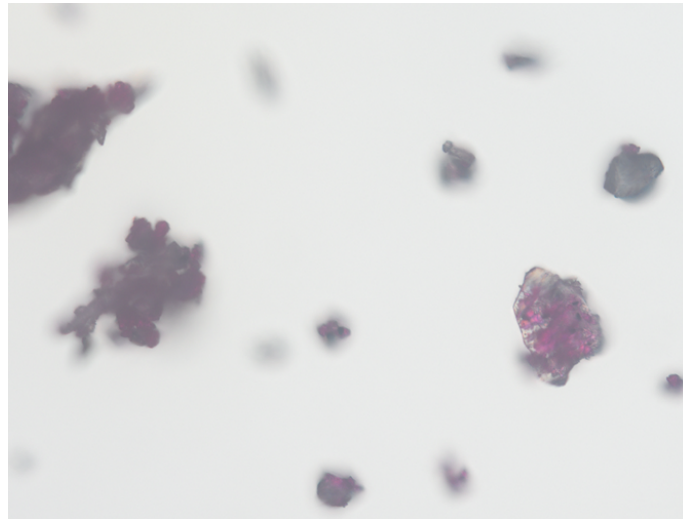


Figure 2.1: Picture of the luminophores under the microscope, optical enlargement 1:100

Results from the microscope inspection show, that they vary in size and shape. They are bright pink in color, which can be seen well on the luminophores on the right side of the picture.

The shape is important to estimate the risk of mechanism failure if the luminophores invade the space between the movable parts of the mechanism. The risk is increased by the uneven surface of the luminophores.

The luminophores used in the experiments were supplied by Partrac in Glasgow. [7]

The variation used in this study is a silt-sized tracer, with a density of 2650 kg/m^3 , a diameter of $60 \text{ }\mu\text{m}$, a pink color, fluorescent and paramagnetic. The request form with the detailed specification can be found in the attachment.

As can be seen in figure 2.1 the luminophores are neither uniform nor round, hence the diameter of $60 \text{ }\mu\text{m}$ can only be an estimate of the average mean.

The sinking velocity of the luminophores is given with $0.013 \pm 0.01 \text{ m/s}$ for luminophores between $60 \text{ }\mu\text{m}$ and $250 \text{ }\mu\text{m}$ and a density of 2600 kg/m^3 [6]. Based on this data, estimates

of the sinking behavior and the spread pattern can be made. To observe this pattern, during the pilot tests for the mechanism in Chapter 4 the sinking behavior is observed. Further considerations regarding the sinking behavior of the luminophores will be made in chapter 3.

The mixing ratio between luminophores and water is given by the experiments carried out by Partrac. One kilogram of tracers is mixed with six liters of water and five milliliters of soap to reduce the surface tension. [6]

2.3 Luminescence

The key phenomenon of luminophores is luminescence. Luminescence is a generic term for various light effects such as fluorescence and phosphorescence. All luminescence phenomena include the ability to glow after being illuminated making them optically distinguishable, even in areas where no natural light occurs. [8]

Every atom has a certain number of electrons that exist on different energetic levels. An interaction can take place between a free photon with a determined frequency and a free electron in the electron shell of an atom. The energy of the photon is absorbed by the atom and transferred to the free electron. [9]

As a result, the electron is brought to a higher energy level. The state is no longer stable for the electron and eventually, it will fall back to its original energy level. Through this movement, energy is released and a photon is emitted. [9]

The purchased luminophores react with fluorescence at a certain wavelength, and the release of energy takes place within 7-10 seconds. If it takes minutes or several hours, it is called phosphorescence. [9]

2.4 Type of result produced by the SPI

As the SPI will be used to collect data, the typically produced results will be explained briefly. With the SPI, it is possible to achieve biological and geological important research results, through measuring a variety of characteristics, including grain size, redox potential, and bioturbation. [10]

A good example of the possible outcomes is shown in figure 2.2. Bioturbation from the surface layers (light brown sediment) into the deeper areas (black sediment) can clearly be seen.



Figure 2.2: Example of a picture taken with the SPI Camera in the German Bay during HE528 with the *RV Heincke* at the long term station H1 by Jennifer Dannheim

To use the SPI as f-SPI, the use of a filter is essential to stimulate fluorescence.

Every optical phenomenon (in this case, luminophore fluorescence) has an optimal wavelength spectrum for its stimulation. The needed light has a wavelength between $\lambda = 275 - 500$ nm which equals violet and blue, but also UV light. That is why, a filter is used for the flashlight. [4]

The filters were purchased from LEE direct, where the filter with the number #713 Winterblue was recommended by M.Solan. [11]

3. Sinking behavior of the luminophores

It is important to know about the sinking behavior of the luminophores to evaluate if the criterion uniform distribution is fulfilled. This includes the sinking velocity, the spreading pattern on the seafloor, and the total time required until the luminophores reach the ground. The data provided by the manufacturer Partrac gives a first approximation. In the datasheet, the sinking velocity for luminophores with a diameter between 60 μm and 250 μm and a density of 2600 kg/m^3 is given as 0.013 ± 0.01 m/s for the luminophores. This is not exactly the data for the luminophores used, but it is a good estimation for a first impression and calculating the Reynolds number (Re). It can be seen that the result ($Re = 0.43$) is well below one.

[12]

$$v_p = \frac{2}{9} \cdot \frac{r^2 \cdot g \cdot (\rho_p - \rho_f)}{\mu} [12] \quad (3.1)$$

$$Re = \frac{\rho_f \cdot u \cdot l}{\mu} [13] \quad (3.2)$$

The used formula symbols are:

- v_p is the sinking velocity, that is meant to be calculated
- r is the radius, half of the diameter, which is given from the technical description with $r = 30 \mu\text{m}$
- g is the acceleration due to gravity, which is given from literature with $g=9.81 \text{ m}/\text{s}^2$ [13]
- ρ is the density of the material, where the ρ_p identifies the density of the particle (2650 kg/m^3 , [6]) while ρ_f identifies the density of the fluid (1038.5 kg/m^3 , [14])
- μ is the viscosity, which is taken from the literature with $1.89 \cdot 10^{-3} \text{ kg}/(\text{m} \cdot \text{s})$ for a salinity of 3.6 ‰ and a temperature of 0°C, which is estimated as the occurring conditions in the arctic deep sea [15]
- u is the sinking velocity for the Reynolds number, which is assumed as 0.013 m/s
- l is the length of the particle, in this case, it equals the diameter and is therefore given with $l = 60 \mu\text{m}$

With the given data, a sinking velocity of $v_p = 0.0146 \text{ m}/\text{s}$ is calculated (the newly calculated Reynolds number is $Re = 0.48$). The result is within the given range for the sinking velocity from Partrac, although the density is slightly higher.

In order not to rely solely on the calculation, the sinking time was stopped during the pilot

tests, which are explained in chapter 4. In the preliminary tests, the distance between the dispensing height of the luminophores and the bottom of the tank was chosen at twelve centimeters. With the sedimentation rate of 14.6 mm/s the expected time until the luminophores reach the ground is around 8.22 seconds. However, this assumption differs from the observation. The first luminophores to reach the ground take about 4 ± 0.1 seconds (human error included), which corresponds to a sedimentation rate of three centimeters per second. This only allows one conclusion: the luminophores stick together. All the other significant values cannot possibly be changed.

Also, it has to be considered the viscosity of water used in the experiment is lower, as fresh water was used with around 10°C water temperature. With different values, the sinking velocity doubles approximately.

It has to be added, that although most of the luminophores reach the bottom after four seconds, the sinking rate is not the same for each luminophore. The tracers have varying velocities and some take much longer. Still, the differences are within the acceptable range. However, the differences align with the observations from chapter 2.2 made under the microscope, where huge variations in shape and size could be seen. The spread pattern will be described further in chapter 4.

3.1 Lateral drift and current

When considering the sinking behavior, the disruptive factors must be taken into account, such as the existing currents near the seafloor. It is expected that the luminophores will drift horizontally. Regarding the current, two different locations have to be considered, because two operations are planned for the LDM.

The first site is located in the German Bight and will be carried out in April 2023. Strong currents have to be expected to occur due to tidal fluctuations. For the deployment, a point in time with high or low tide should be chosen since the current is expected to be the lowest then. Drift is still expected, as it cannot be worked precise enough.

The second location will be located in the Arctic deep sea where experiments will be carried out in 2024. Experiments by C.Hasemann prove a current in depths of 2600 m. At a distance of one meter above the seafloor, a velocity of 4.6 cm/s, and at a distance of 2.5 m a velocity of 5.4 cm/s were measured. [5]

A model for the current velocity on a wall is the logarithmic wall law. The required formulas are:

$$u = u_\tau \cdot \left(\frac{1}{\kappa} \cdot \ln\left(\frac{y \cdot u_\tau}{\nu}\right) + C_1 \right) [13] \quad (3.3)$$

$$u_\tau = \sqrt{\frac{\tau_w}{\rho}} [13] \quad (3.4)$$

$$\tau_w \sim \sqrt{\frac{\mu \cdot \rho \cdot u_\infty^3}{x}} [16] \quad (3.5)$$

The used formula symbols are:

- u is the velocity of the current, which is calculated
- u_τ is the wall shear stress velocity, which is dependent on the wall shear stress [13]
- κ is the Karman constant, which is given by literature with 0.417 [13]

- C_1 is the integration constant, which is given with 5.5 from the literature [13]
- y is the distance from the sea floor, which is the variable in this case
- μ is the kinematic viscosity, which is taken from the literature with $1.89 \cdot 10^{-3} \text{kg/m}\cdot\text{s}$ for a salinity of 3.6 ‰ and a temperature of 0°C , which are estimated as the given values in the Arctic deep sea [15]
- ν is the dynamic viscosity, which can be calculated from the kinematic viscosity with $\mu/\rho = \nu$
- ρ is the density of seawater, which is taken from literature with the average density of seawater (for the deeper sea) of $1038.5 \pm 2.4 \text{kg/m}^3$ [14]
- τ_w is the wall shear stress
- u_∞ is the free water current, which is not influenced by the wall
- x is the length of the wall which influences the current

Two important variables that are not given in the literature values are the length of the wall and the free current, which is uninfluenced from the seafloor. For the free current data from experiments in the Fram Strait at a depth of about 2,600 m, were taken as 5.6 cm/s. [5]

It has to be kept in mind, that much stronger currents could occur, but this is not considered very likely and hence not implemented in this study. It also depends on the direction from which the current comes.

The wall length is estimated to be 100 m. This is the most difficult value to estimate because it is highly dependent on the seafloor structure and the depth profile. It has to be mentioned that for a length of 10 m, the calculated lateral drift is doubled, and is cut in half for a length of 1000 m. The calculation with the results shown in figure 3.1 and table 3.1 were made with $x=100$ m.

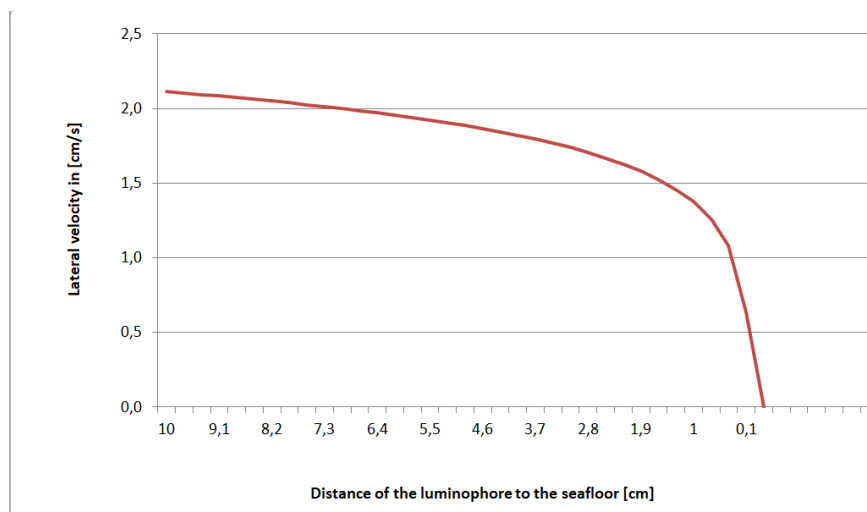


Figure 3.1: Lateral current depending on the distance of the luminophores to the seafloor

The logarithmic structure from the graph in figure 3.1 is visible. The formula is not valid near zero, since the corresponding value for $y=0$ is $u = -\infty$. Therefore the last value is not chosen as zero. [13]

The calculations are made with 120 mm distance between the seafloor and the LDM, to tie in with the conditions from the preliminary tests.

To create the graph of figure 3.1, time intervals of 100 ms were used. For a better understanding of how the total lateral drift was calculated from the lateral velocity, the calculation is presented in tabular form in table 3.1. The selected interval for the table is 400 ms.

Table 3.1: Calculation of the lateral drift depending on the time

Time	Distance to the seafloor	Lateral velocity u	Lateral drift
0 s	120 mm	21.7 mm/s	0.0 mm
0.4 s	108 mm	21.4 mm/s	16.5 mm
0.8 s	96 mm	21.0 mm/s	17.0 mm
1.2 s	84 mm	20.6 mm/s	25.2 mm
1.6 s	72 mm	20.1 mm/s	33.2 mm
2.0 s	60 mm	19.5 mm/s	41.0 mm
2.4 s	48 mm	18.8 mm/s	48.5 mm
2.8 s	36 mm	17.9 mm/s	55.7 mm
3.2 s	24 mm	16.6 mm/s	62.3 mm
3.6 s	12 mm	14.3 mm/s	68.0 mm
3.99 s	0.3 mm	0.0 mm/s	68.0 mm

To calculate the total lateral drift, it is necessary to integrate the velocity over time. Since the sinking velocity is known from the tests, a function of the distance to the seafloor versus time was created. The distance of the luminophores to the seafloor is $f(t) = 120 \text{ mm} - \text{time} \cdot 30 \text{ mm/s}$, and selected values from the function are shown in table 3.1.

With the estimates made and the values known from the literature, the lateral velocity u can be calculated depending on the distance of the luminophores to the seafloor. The column for the calculated velocity can be seen in table 3.1 next to the distance to the seafloor.

The lateral drift is calculated through a partial integration (multiplying the time interval by the corresponding velocity). The result is the lateral drift as a function of time.

The last value in the lateral drift column is the significant value, which indicates the total lateral drift. With the made estimates, the result is 68 mm drift. For a total length of the mechanism of 240 mm, this equals less than a third of the total length and less than a fifth of the window length. The lateral drift is considered acceptable as it covers most of the SPI window.

However, it should not exceed the calculated value. For a better result, the distance to the seafloor is set to 100 mm resulting in a calculated drift of 59 mm. To not disturb the organisms operating on the seafloor, the distance cannot be reduced any further.

4. Preliminary tests for different dispensing mechanisms

The requirement for the mechanism was to distribute the tracers evenly over an area of approximately 250 mm x 150 mm. The thickness of this distributed layer was determined to be 3 mm.

Although the glass window is only 150 mm wide, 50 mm overlength is provided on both sides of the glass window to ensure that the cross-entry of organisms is also visible. For the same reason, the area is defined up to a distance of 150 mm from the glass window. However, the biggest challenge in the development of this mechanism is the change between the tracer-containing state and the tracer release state. Here a trigger motion has to be developed to change from one state to another.

4.1 Planning

Based on the initial ideas, sketches and 3D models were developed in the design software from Autodesk Inventor. [17]

It was decided to use 3-D printing for the manufacturing of the prototypes, as it is time efficient and convenient for small quantities.

The size of the prototypes is not the same as the size that will be used for the final design to reduce the used material and time. The sample versions were chosen with 60 mm x100 mm for the grid with hopper and 100 mm x100 mm for the movable grids. In addition to the evaluation of the different mechanisms, the sinking behavior of the luminophores was observed. It is important to know the sinking velocity and to get an idea of the spreading pattern, to decide whether the condition for an even distribution is fulfilled.

4.2 Criteria

Preliminary tests were carried out to investigate the best dispensing method. Based on the results, the final design will be selected. In order to decide well-founded, the ideas are going to be judged by certain criteria.

- The first criterion is to design a mechanism that works as simply as possible. This is probably the most important criterion, as it results in low cost, **easy application**, an **easy movement**, and a less time intense production.
- A **high dispersion rate** of the luminophores is needed, in order to use the tracers efficiently. Due to the turbulence of the water and the current, a high percentage is expected to not reach the area in front of the glass window.
- **No risk of jamming** is wanted, as remaining luminophores would not only be a waste but also a risk.

- As a risk analysis to avoid malfunction, it is important to consider problems that might occur in the future. The expected effort for further developing of the prototype includes a **method for the movement** and the possibility of **pressure equalization**.
- **Flushing of the tracers from the mechanism has to be avoided.** While the SPI is lowered, the water flow could wash the luminophores out of the container. Pressure can be used to seal the container watertight. This stands in contrast with pressure equalization, as the latter can be realized easily if water can get into the mechanism.

4.3 Ideas for the mechanism

Several ideas were considered. Based on the 'salt-shaker' type used in the AWI experiment from 2015, a grid was chosen as the outlet. In addition, a closing mechanism had to be added to the grid. [2]

Two methods were chosen as they best met the basic requirements. They will be explained in detail from their Inventor models in the following subsections 4.3.1 and 4.3.2.

4.3.1 Two movable grids

The key idea is to design two grids, moving against each other, to be seen in figure 4.1. Different colors are used for a better understanding of the single components. The upper grid (1), and the lower grid (2) are designed the same, only the lower grid has extrusions to two opposite sides. A lead component (3) can be screwed onto these extrusions. This ensures a straight line of movement and also allows pressure to be applied.

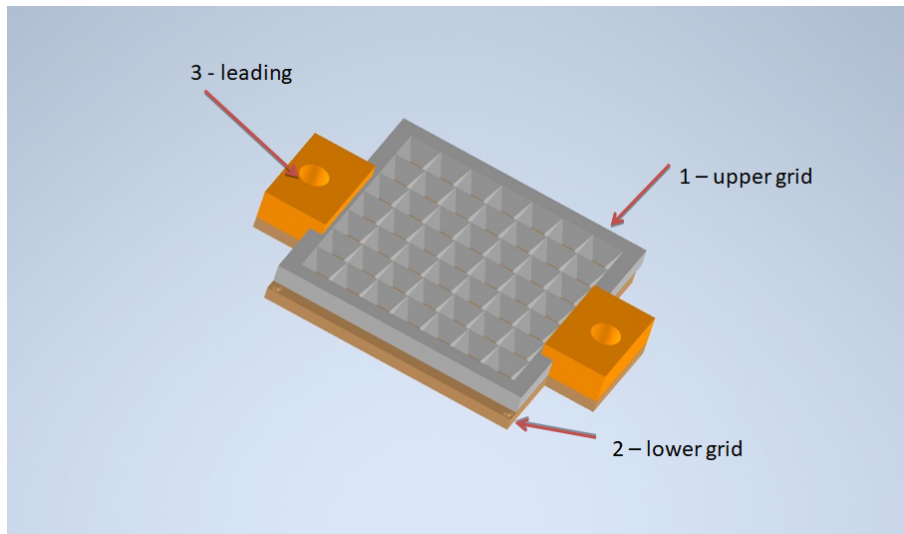


Figure 4.1: Preliminary test, method 1: Two movable grids, Inventor Sketch

Thus, the openings can either be aligned on top of each other creating permeability, or the openings can be blocked completely. Cones around the holes ensure that all the surface area leads to the openings while the holes still are small enough to be sealed by the other grid. This way the grids are sealed during the luminophore-containing state.

A rack is added for stability. Since there are already screws needed to mount the lead, the same screws are used to mount the mechanism on the rack which consists of a thick plate (15 mm) on each side a rack. This can be seen in figure 4.3. The movement is realized manually.

4.3.2 Grid with movable hopper

The idea of a grid with a movable hopper consists out of two components, shown in figure 4.2. The hopper (1) is the movable component. In the initial position, the hopper is placed on the board (2) on a part without holes. The board also contains the grid. This start position prevents the tracer from dispensing too early. To prevent a sideways movement of the hopper and to ensure that it is moved in a straight, rather than a zigzag line, a leading is included as seen at number two. Lastly, number three in figure 4.2 labels the grid.

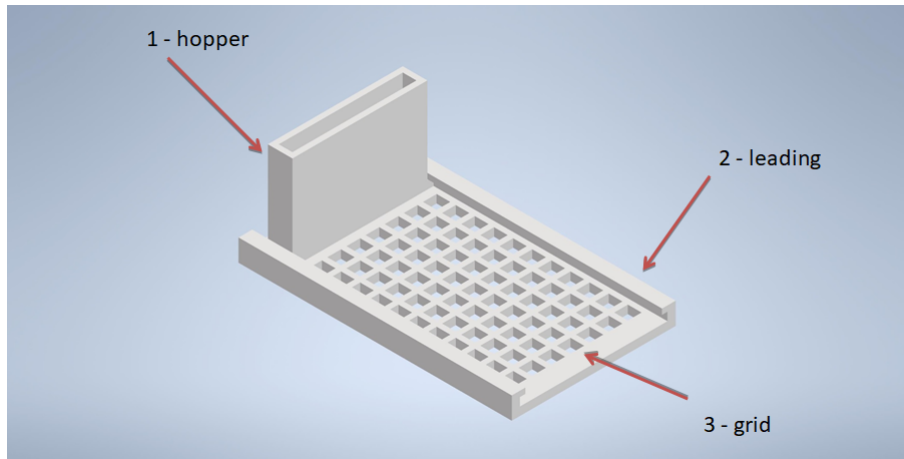


Figure 4.2: Preliminary test, method 2: Grid with movable hopper, Inventor Sketch

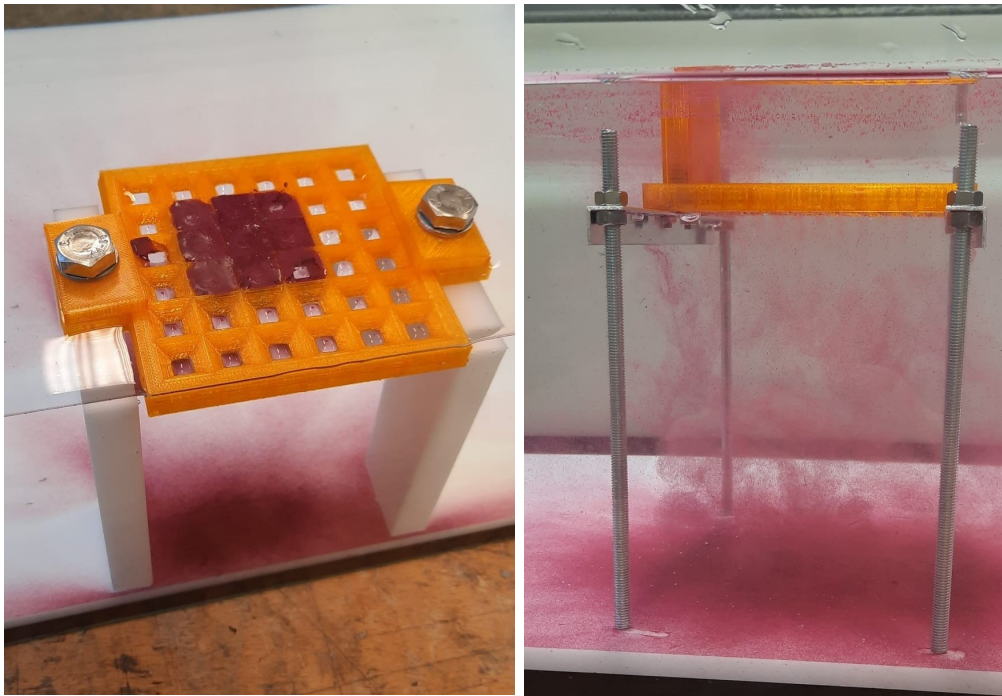
The movement was carried out manually by dragging the hopper from the now left side in figure 4.2 to the right side.

The rack consists of two L-sections, screwed into the short ends of the mechanism. At some distance to the grid, four rods are mounted. The rods maintain the grid's height to the aquarium's bottom.

4.4 Implementation

Both mechanisms have been tested in water. An aquarium was chosen as the water container. The volume was large enough to allow free sinking without requiring too much water. For the experiment, the luminophores were mixed with some water, as this is recommended by the producer, though the ratio was higher (one to one) than recommended, as the mixture would have been far too liquid otherwise for our application. No soap was used, as it could affect the organisms later during the test in the North Sea.[6]

The aquarium was filled up so that the water level aligned to the height of the luminophores in the particular mechanisms. Both mechanisms were moved manually. The results can be seen in figure 4.3.



(a) Method 1, two movable grids, during the practical test

(b) Method 2, grid with hopper, during the practical test

Figure 4.3: Comparing the two methods after the preliminary tests, pink luminophores were dispensed out of the prototypes (seen in orange)

One difference that was noticed is the path of the motion. While the hopper has to be moved around 90 mm, method one only requires a movement of 5 mm, through the lower grid. Maintaining the same velocity for the hopper while moving it over the grid was impossible. Not only did it jam on the leads but also the tracers remained on the grid. In addition, remnants of the luminophores stayed in the container.

The spreading pattern is seen nicely in figure 4.3b. The luminophores appear to have spread evenly, at least to the human eye. No structure from the grid was transferred onto the ground, it is not visible where the openings of the grid have been. As the grid with hopper experiment was carried out secondly, the rack was designed in a manner that the luminophores could sink freely. They appeared to spread to the same amount in every direction. Furthermore, it was found that around four seconds are needed for the majority of the luminophores to reach the ground. The movement of the dispensing luminophores can be described as tiny clouds, to be seen in figure 4.3b. For the two grids, a lot of force was needed for the movement, due to the applied pressure by the two screws seen in figure 4.3a. Some luminophores were not dispensed, but remained in the mechanism, also to be seen nicely in figure 4.3a in the upper grid.

4.5 Evaluation

Both methods have been judged based on the mentioned criteria. Depending on the fulfillment of the criteria, a distinction was made between good, medium, and poor. The following table 4.1 shows the results. Possible future problems will be discussed in more detail in this section. Based on the results one mechanism is selected.

Table 4.1: Evaluation table for the two mechanisms

Criteria	Grid with movable hopper	Two movable grids
Easy application	Good	Good
Easy movement	Medium	Good
High dispersion	Good	Good
No jamming	Poor	Medium
Equal dispersion over the area	Medium	Good
Avoiding flushing out	Poor	Medium
Problems for future (such as)	Medium	Good
Low expected effort	Medium	Good
Easy method for movement	Poor	Good
Pressure equalisation	Good	Medium

Categories that are valued as good will not be discussed, as they are not likely to cause difficulties in the future. First, it will be looked at the result of the grid with the movable hopper.

The movement caused problems because it was not possible to maintain a constant velocity. A lot of force was needed, because the edge of the hopper would stick to the lead component. The category no jamming was correspondingly not fulfilled. Also, the tracers remained on the grid, causing additional seizures.

The equal dispersion could be influenced by the jamming and the different speeds, especially if the movement would be over a longer distance. In this case, the sinking behavior almost eliminates any indifference.

The future problems are structured into three main categories. The expected effort is higher in terms of the motion. In order to contain the same velocity an attenuation will be needed. In the experiment, the hopper was moved several times from one end to the other end. This will not be possible for the mechanism. There would have to be a solution for the seizure.

Pressure equalization could be achieved with an elastic lid for the hopper. However, depending on the velocity and the dispensing rate, it may be necessary to apply external pressure to the lid to accelerate the dispensing process. This could stand in conflict with the flexible lid.

Furthermore, the bottom end of the hopper would need to be sealed. This could be done through pressure application, which would hinder the movement of the hopper even more. As this is manageable, but possibly a lot of effort, the future problems are rated as medium.

Secondly, the two movable grids are evaluated. The jamming was a minor problem. Since the side of the grid without the cones was printed with a supporting structure they had to be filed down, increasing the friction coefficient. Therefore more force was required. The pressure was exerted by the screws and the lead element, further complicating the movement. A connecting board could be integrated for a better friction coefficient between the upper and the lower grid.

For a continuation of this method, it is necessary to look at the movement. Since the movement is short, no constant speed is needed. The expected effort is relatively low, a container for the tracers would need to be added as well as a system for the movement. Pressure is already applied, which seals the two grids against one another and prevents the luminophores from being washed out by the current. The lid of the yet-to-be-added container could serve as an inlet for water, to enable pressure equalization. To let water enter and prevent luminophores from washing out, a labyrinth seal can be a solution. The principle of two movable grids is chosen for the final design, because of the discussed advantages.

The design details are discussed further in chapter 5

5. Basic design

From the first design of the preliminary test, some alterations must be made to adjust the basic idea regarding size, trigger, activator for the movement, and attachments for mounting. Not only the mechanism itself is explained in this chapter, but also the mounting to the frame of the SPI as well as the activator for opening the mechanism.

For a better understanding, the single components are not explained individually, but rather in their assembled state. Thus, the components can be understood directly in the context of the overall concept. In addition, the technical drawings can be found in the appendix, to get a detailed insight. Excluded from this are the upper and the lower grid. As they were printed, no technical drawing was made.

It has to be taken into account, that the shown mechanism in the figures is already altered for the chosen trigger, which will be discussed in chapter 6.

5.1 Material and manufacturing

Firstly, the manufacturing methods and the used material will be discussed, as they influenced the design choices to a certain degree. Making components producible with water jet cutting has to be considered during the design.

The manufacturing and assembly of the LDM components were carried out in the AWI workshops. In this study 3D-printing and water jet cutting were the main methods used to manufacture the single components.

5.1.1 Manufacturing

The upper grid and the lower grid were printed, because the rectangular shape of the cones could not be manufactured using conventional methods such as countersinking. 3D-printing is a standard technique and is commonly used. From the Inventor sketches, the file format has to be changed once before it can be sent directly to the printer.

All other components were manufactured using water jet cutting and manual finishing. The advantage of water jet cutting lies in its time efficiency, as 3D printing a single component can take up to 26 hours, as was the case for the upper grid. In order to manufacture the not printed components, engineering drawings must be created. In the appendix, technical drawings can be seen for all components that were water jet cut.

5.1.2 Material

The mechanism as a whole has no compression-resistant parts, therefore no high yield point was needed of the material. More specifically, this means that hollow parts are not filled with air. The material only has to withstand its own direct compression. Since solid material is not compressible, a low yield point is sufficient.

Polymers in general are less time and cost intense to manufacture than metals. They are suitable for long-term use in seawater, as they have a low corrosion potential. Hence they were used for the LDM. As screws from stainless steel provide more stability and also have

sufficient corrosion resistance for the application, they were the exception.

A common material for 3D-printing is Polylactide (PLA), which was used in the color black for all printed parts.

The other components were produced from Polyoxymethylene (POM). POM is also known as polyacetal and provides good mechanical properties. Additionally, they can be used at low temperatures.[18]

The advantages of polymers in general are their high corrosion resistance, as well as their low price and high availability.

5.2 Mechanism

In total, the mechanism consists of four separate components: The upper grid, the lower grid, the connecting component between the upper and the lower grid (to provide a better friction coefficient), and a lid for the luminophore container. All components are marked in different colors for a better overview. The mechanism is shown from above in figure 5.1.

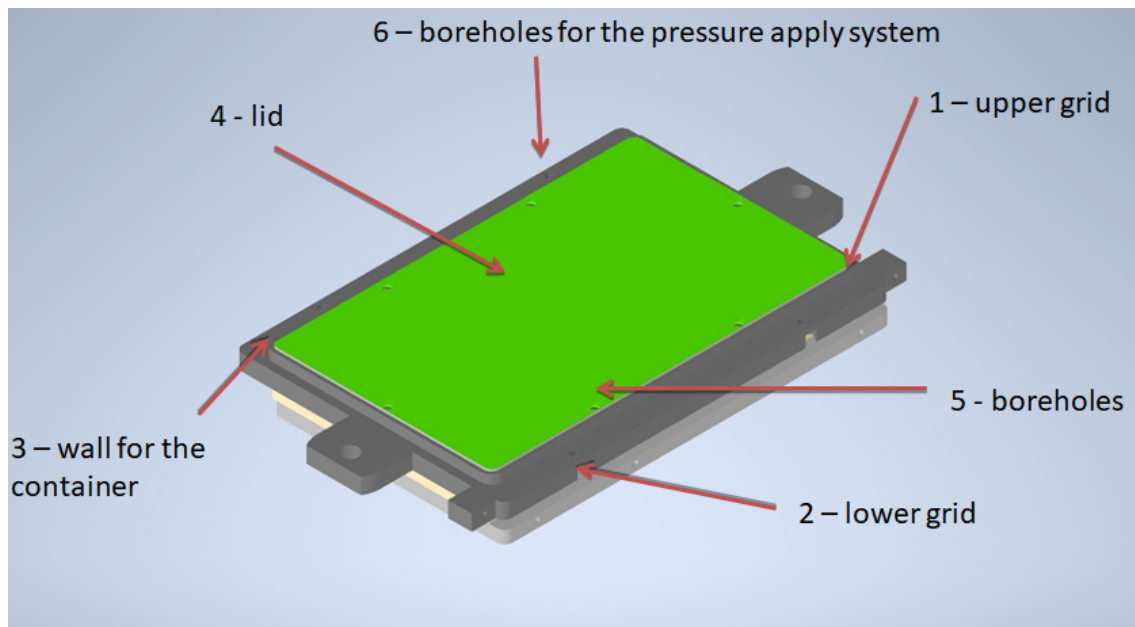


Figure 5.1: Finished LDM, view of the mechanism from above, Inventor model

The upper grid (1), shown in a dark gray color, and the lower grid (2), shown in a light gray color, are the main component. The basic design of the grid was explained in chapter 4. This includes the cones around the holes, which lay below the lid (4). The lid can also be seen as a technical drawing in the Appendix LDM - 004.

For a complete understanding of the LDM, the view from the bottom is shown in figure 5.2.

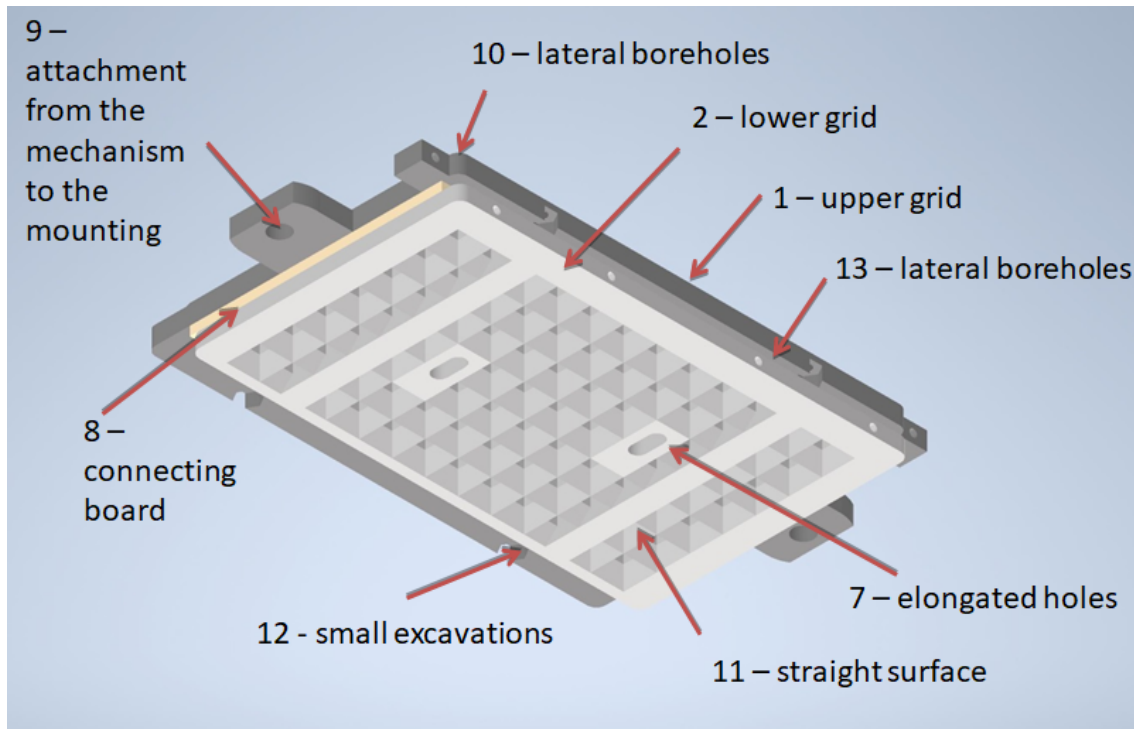


Figure 5.2: Finished LDM, view from the bottom, Inventor model

The upper grid is 10 mm thick. The holes are 5 mm x 5 mm, while the upper cone area is 18 mm x 18 mm on the opposite side. This creates an angle of 57° for the chamfer.

The wall for the container (3) can be seen surrounding the lid in figure 5.1. It is included in the upper grid, consisting of the wall with a bearing surface at the height of 2.82 mm on which the lid can be placed.

The luminophores can hence be stored exactly above the grid so that they can be dispensed when opened. The created volume corresponds exactly with the wanted 150 mm x 250 mm x 3 mm plus 20% extra. While the container itself, as well as the grid, is smaller than the designated distribution area (137 mm x 245 mm) in order to correlate with a full number of cones and openings, the wanted area can still be covered through distribution. It was seen in the preliminary tests, that an area far larger is covered by the opening than the opening itself.

As the view is blocked in figure 5.1, the upper grid is additionally shown individually in figure 5.3.

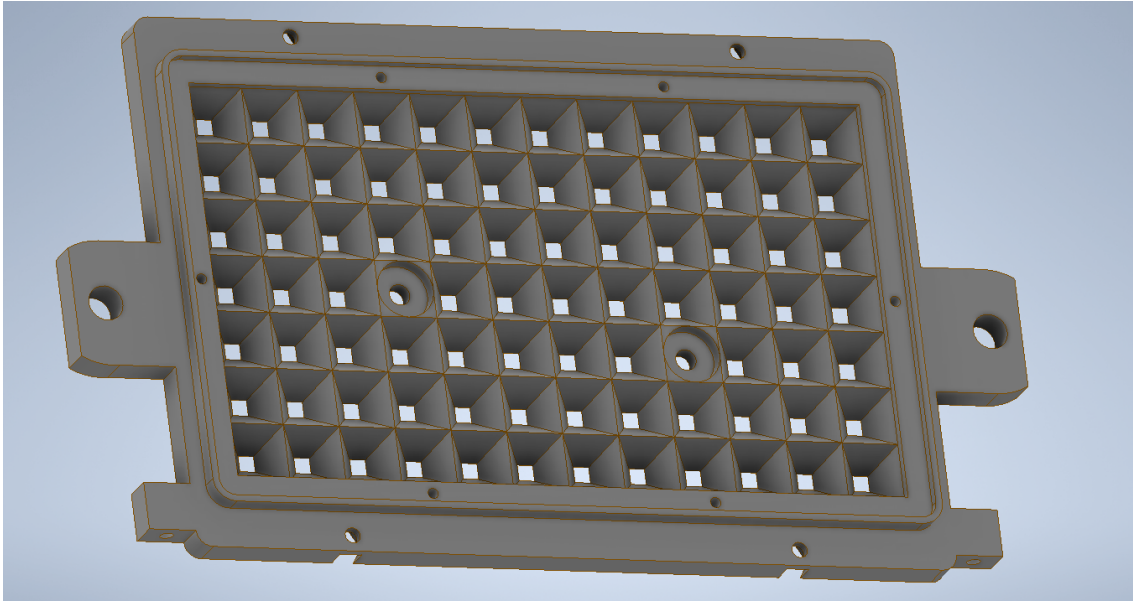


Figure 5.3: Upper Grid, view from above

Boreholes (5) ensure that the lid can be screwed to the shoulder of the wall. This creates the simplest type of labyrinth seal, preventing the luminophores from being washed out while allowing water to enter. There are six screws.

A little hard to see are the boreholes for a pressure application system (6). By applying pressure, the bottom of the container is sealed watertight. This will be discussed in more detail in chapter 6.

Figure 5.2 again shows the upper grid (1) and the lower grid (2) as well. The cones with holes in the middle are visible in the lower grid. It is 8 mm thick, and as the angle of the cones is not as important on this side, 45° was chosen.

Two of the square holes have been replaced by elongated holes (7), 18 mm apart. Guiding screws are added to these holes to provide leading for the movement of the lower grid. As the length of the movement is determined, provides a stopping point, so that the openings of the grids align. The upper grid has matching bearings so that the lower grid can be moved against the upper one.

The connecting board (8) is a simple POM board with holes in it, that match the openings of the grids. For stability, frames are added to the lower grid, which fits exactly into the holes of the connecting board. Mainly, the connecting component was added to improve the friction coefficient between the upper and the lower grid. The technical drawing LDM-003 in the appendix belongs to the connecting board.

Due to a manufacturing problem, ultimately the connecting component was left out. The friction will be between two printed PLA boards (upper and lower grid), which will be calculated in section 6.5.

Since the lower grid was chosen to be the moving one, the attachment of the mechanism to the mounting (9) is provided via the top grid. The mounting is the connecting component between the SPI and the LDM. Therefore, it will be explained in more detailed in section 5.3.

Other numbers refer to parts that have already been modified to fit the trigger. They will be explained briefly.

A straight surface (11) can be used to apply pressure to the lower grid. This would have been difficult to realize on a non-existent surface. The small excavations (12) are meant for screw nuts, corresponding with the holes from figure 5.1 (6). Finally, lateral boreholes (13

and 10) are used as a leading trigger for lateral movement. This will be explained further in section 5.4.

5.3 Mounting

The mount design is made to attach the mechanism to the SPI as it will be used during the experiments in the North Sea. For further use, the SPI will be attached to a lander, eliminating the need to be anchored separately.

Since both sides are the same, the construction is symmetrical. The mounting is shown in the built together condition with a space in the middle, where the LDM would be.

Figure 5.4 shows the brackets (1), which are attached to the rack of the SPI. The SPI is explained more detailed in section 7.3 and is shown in figure 7.2. Two brackets allow an attachment of mounting to the rod of the rack. Additionally, they can be moved along the rack. The boreholes connect the brackets (2) to the connecting element (3). The technical drawings of the brackets (LDM-Halterung 01) and the connecting element (LDM-Halterung 03) can be found in the appendix.

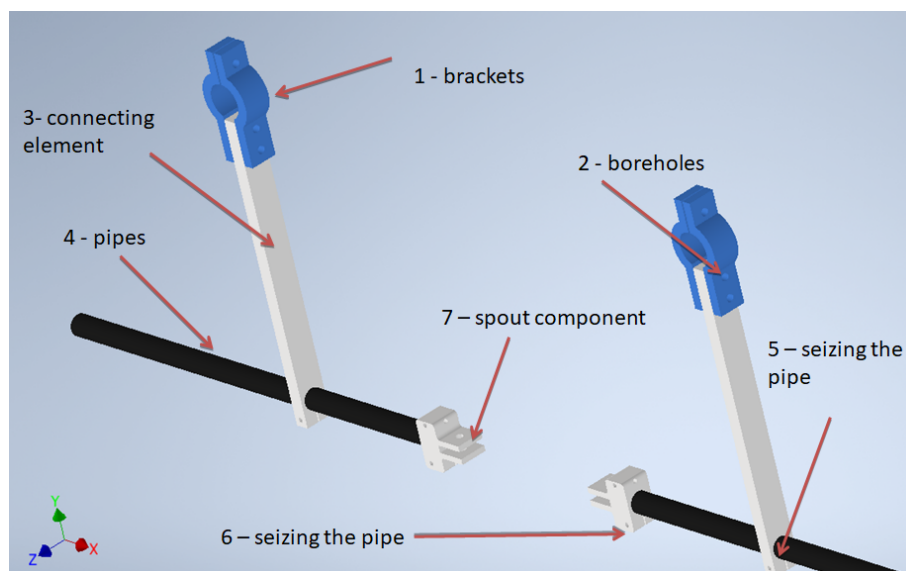


Figure 5.4: View of the mounting, Inventor model

Pipes of carbon fiber-reinforced plastic bridge the distance between the two sides of the rack and the mechanism in the center. In figure 5.4 the pipes (4) are not fitted to the right length, so this can be adjusted manually. Number five and number six both show the clamping principle of the connecting element (5) and the spout component (6). The spout component can be seen in the appendix as LDM - Halterung 02.

5.4 Activator

Based on the preliminary tests as well as the general assignment, motion must be included. In order to keep the mechanism simple, the movement is mechanically activated. Spring tension was determined because it was used in similar devices (see section 5.4.1). It is a simple way to create a force large enough to move the lower grid. For a more precise lead, compression springs were chosen.

5.4.1 Basis from the literature

The idea to use compression springs is based on similar developments. For a water sampler, a piston needs to be moved within a cylinder. The change between the two positions is released with extension springs, purely mechanical. Since the activator realizes a similar change between two positions, the idea of using springs was adopted. However, it was decided to use compression springs, as this was as well the original idea for the water sampler. [19]

5.4.2 Activator explained

The activator is shown in figure 5.5 implemented on the left side of the mechanism to provide some context.

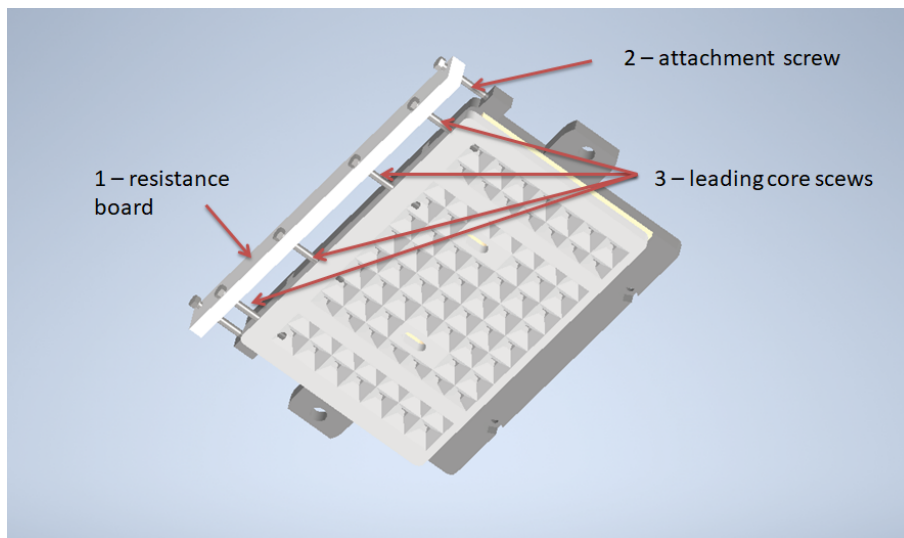


Figure 5.5: View of the activator, Inventor model

The resistance board (1), shown on the left side in figure 5.5, and the screws, shown connecting the resistance board to the mechanism, are the main components. There is a screw at each end that acts as an attachment screw (2) to keep the resistance board at a constant distance from the upper part of the mechanism. The board is compressing the springs, as they cannot fit the full length of the screws.

The four screws in the center act as the leading core (3) for pressure springs. The compression springs will be compressed to a certain length, applying force to the lower part of the mechanism. The core screws are not attached to the resistance board, but only to the lower grid, so that they can move freely with the lower grid. When the lower part of the mechanism is no longer blocked in its movement, the springs can elongate and the kernel releases their force.

6. Trigger

As explained in section 5.4 a consistently applied force is used to open the mechanism. In order to prevent the LDM from opening before the allotted time, a secure locking of the mechanism must be implemented.

In addition to blocking the motion, pressure must be applied to the mechanism as discussed in section 4.5. As both requirements are intended to prevent movement, they are combined. By applying pressure, the movement of the LDM can be blocked completely.

Different ideas were considered. One option would have been to implement a barrier, such as a bolt, for instance, that pierces through the upper grid to hinder the lower grid from moving. This can still be done as an additional measure. However, additional pressure would have to be applied to prevent the luminophore-water mixture from spilling out. Therefore it was considered easier to use the trigger to apply pressure as well.

Moreover, freezing the luminophore-water mixture was also considered. The advantage is that no pressure would have had to be applied. On the other hand, the main problem would have been the melting of the luminophore-water mixture. As the LDM will be used in the Arctic deep sea, water temperatures at the freezing point are expected, which would result in slow melting or even no melting at all. Therefore, these two ideas were ruled out and it is continued with pressure-applying methods.

6.1 Type of Trigger

There are three main ways to realize the trigger: mechanical, electrical or chemical.

A mechanical trigger needs a certain amount of movement for a reliable release. In this case, the prism of the SPI provides mechanical movement. The idea is, to design a kind of hook, which is fastened on the prism. When the prism moves into the sediment, the hook is pulled out.

What might be problematic is the turbulence in the sediment. The moment the prism moves into the sediment, it will be swirled up, creating turbulence. This will affect the sinking behavior of the luminophores in an unpredictable way.

An electrical trigger would provide a precise point of time for the trigger. The movement is clearly determined and precise. The circuit would be quite simple, with only a clock timer, a battery, and a motor for the movement. However, the electrical components would have to be packed watertight, resulting in a titanium case or a thick stainless steel case for the deep sea. This can be expensive. The effort of designing a watertight case is seen as unnecessary for this application.

Combining the electrical and the chemical solution would result in a burning wire. Applying electricity to a metal, electrochemical corrosion is triggered. However, a power supply would still be necessary. Therefore, the same problems as for the electrical solution appear.

A chemical trigger works through corrosion. Although electrochemical corrosion is the most common type, pure chemical corrosion also exists and does not require electricity of any kind. Salt water is sufficient for activation. Since there is a company providing such

a product (Galvanic Time Releases from International Fishing Devices Inc.), the effort is relatively low. In figure 6.1 a selection from the product range is shown.



Figure 6.1: Product range of galvanic time release, the upper row shows releasing time ranging from 1 day to 14 days, the lower row shows costume releases ranging from one hour to 100 days [20]

The company offers several options, whereas a release after one day is what would be needed for an application in the deep sea. Of course, salinity and temperature must also be taken into account for the dimensioning.

Due to the different applications (in the North Sea and in the deep sea), two different triggers can be used.

While the experiment in the North Sea will only last five hours, a Galvanic Time Release is not optimal, because it takes too long to dissipate. Here, the mechanical trigger can be used, to release the luminophores as quickly as possible. Turbulence is a disrupting factor that prevents an even spread pattern. Nonetheless, the experiment is mainly to control the LDM rather than to observe the bioturbation of the North Sea.

For the second application in the deep sea, a Galvanic Time Release is highly recommended, as it is the least intrusive. It is easy to use, is activated after 24 hours when the sediment has settled, and can be replaced without difficulty. Also, with a cost of around 10 \$, the price is relatively inexpensive. [20]

Moreover, it has been used for over 30 years in mostly fishery applications, but also in research. [21]

6.2 Criteria

Comparison criteria were identified to evaluate the systems. On this basis, the various ideas were evaluated and a selection was made.

- The pressure application is wanted with an **easy-to-understand user application** and little effort in production.
- Since galvanic time release was chosen as the chemical trigger, it is important that the ideas **can be realized with galvanic time release**.
- Pressure is applied not only to prevent the luminophores from being rinsed out and water entering but also to prevent water leaking out when still on land but already filled. Therefore, it would be ideal if the **pressure could be applied prior to the filling of the mechanism**.
- It should be made sure, that **no openings are blocked by the trigger**.

- To get a more accurate idea of the forces required, it would be helpful **if the pressure was calculable** without great effort.

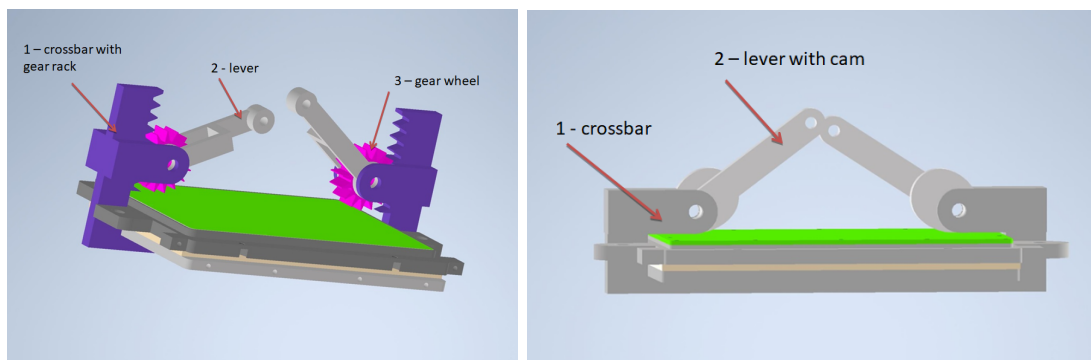
6.3 Ideas

In order to find the best solution for applying pressure to the mechanism, ideas were developed and compared. Each idea could be very similar to one another, with only small alterations made for improvement. The most important ideas are divided into two groups of similar approaches and discussed together in the following section.

6.3.1 Pressure application through levers

This approach is mainly focused on user-friendliness, providing levers, which connect easily. When bringing the levers into a horizontal position, force is created and the mechanism is compressed.

The disadvantages are that most of the applied force is generated on top of the lid, which can cause difficulties as the space below this point is hollow. Further, a pressure application before a filling is impossible for these two variations of the same method.



(a) Draft one: simple gear, Inventor model (b) Draft two: lever with cam, Inventor model

Figure 6.2: Methods to apply pressure to the LDM with lever systems

Figure 6.2a shows three components. The crossbar, connected to a gear rack (1) provides stability. Due to the mounting, connecting the LDM to the SPI, the crossbar cannot be placed centrally.

In addition, the crossbar is extended upwards to support the lever (2) and the gear wheel(3). Both levers can be connected through the hole at their ends if they are horizontal. The connection is made with a Galvanic Time Release. As soon as it corrodes, the levers pop open and the pressure is released.

The improved idea is less complicated and can be seen in figure 6.2b. Instead of a gear system, a cam (2) is used on both sides. By the movement, the extended part which holds the lever (1) is pressed further away from the mechanism, while the crossbar is pressed into the mechanism. As each cam can be moved freely, pressure can be created with the force of the cam and the crossbar as counterresistance.

6.3.2 Pressure application through springs

As compression springs were used in the activator, the idea was developed to use compression springs as well for the trigger. It is less user-friendly, as each spring must be fixed into a position individually. Advantageous is the more precise calculation of the springs. Also,

the container can be filled, after pressure is applied.

Two designs were made, whereas draft four is a continuation of draft three. Both can be seen in figure 6.3.

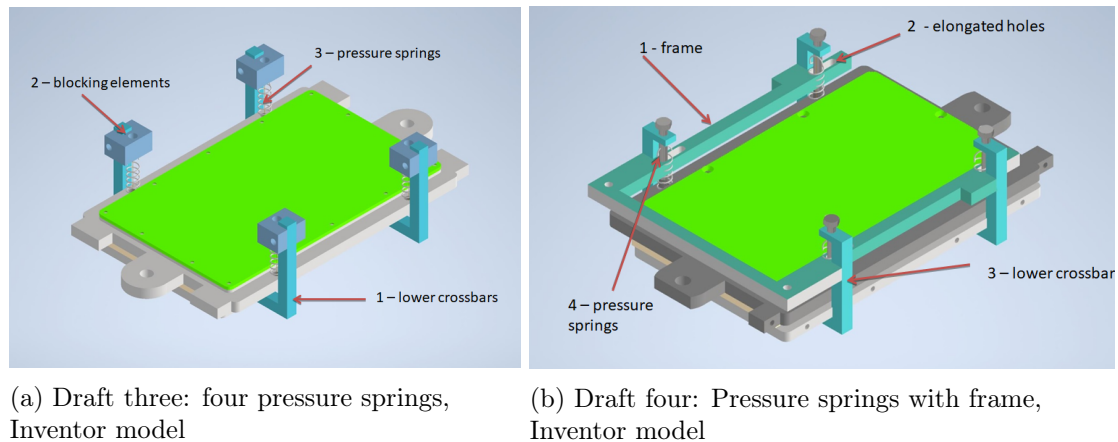


Figure 6.3: Ideas with elastic springs

In figure 6.3a, three arrows indicate the lower crossbars with extensions to the top (1), the blocking elements to fix the compression of the springs (2) and the elastic springs (3).

Each spring is compressed by a blocking element. They can be fixed to the extensions of the crossbar at a certain height and fasted with Galvanic Time Releasers.

Contrary to the two first ideas, four triggers are needed. As the chemical reaction is not precise, it is assumed that they will corrode at different rates, creating a misalignment in the spring decompression.

A solution to that is idea four, shown in figure 6.3b. The most important addition is a frame (1). Elastic springs are now constrained by the frame all at the same time. Extensions of the crossbar (3) secure the frame with bolts, blocking movements upwards. When the frame is moved to the left, elongated holes (2) ensure that the screws (4) do not block the movement.

The blocking takes place in only one of the bolts, which is longer than the rest so that it can be secured with a Galvanic Time Release. With an elastic band, the frame is exposed to a force and gets pulled sideways, as soon as the releaser has corroded.

6.4 Decision

Based on the criteria which were explained in chapter 6.2, a trigger is chosen. For a better overview, each idea has been rated as good, medium, and poor according to the fulfillment of the criteria. The results are shown in table 6.1.

Table 6.1: Criteria for the trigger system

Criteria	Draft one	Draft two	Draft three	Draft four
Easy user application	Good	Good	Good	Good
Viable with one galvanic time release	Good	Good	Poor	Good
Calculable pressure	Poor	Poor	Good	Good
Pressure application	Poor	Poor	Good	Good
viable before filling the container	Poor	Poor	Good	Good
blocking the openings	Medium	Medium	Good	Good

All methods are viable with Galvanic Time Release. For drafts one and two, the levers must be brought to a horizontal position and be connected to the Galvanic Time Release. For drafts three and four, the springs have to be compressed with blocking elements, which are then connected to the frame with the Galvanic Time Release.

Additionally, a frame has to be installed for draft four.

Each solution can be fixed into its place with a Galvanic Time Release. Problematic is the use of multiple Galvanic Time Releases because they cannot be expected to dissolve at the exact same time. This complicates the precise pressure design of the lateral activator.

In draft four the frame blocks all four pressure springs simultaneously, solving the problem of all springs being activated at the same time.

It is also important to consider that the trigger mechanism may partially block the openings of the lower grid since a counter-bearing is needed for support. As it is not crucial for the openings in the lower mechanism to have funnels, they can be omitted and a flat surface can be created. However, since the plate is moving over the short axis, the crossbar in drafts one and two would partly cover some openings due to the movement. It also might get pulled with the lower board.

This cannot happen with drafts three and four, because the direction of the movement is crosswise to the bars of the trigger.

Based on these criteria, draft four was chosen, even though using the frame means some extra effort. But the advantage is the exact feasibility and safety factor.

The finished manufactured LDM can be seen in figure 6.4.

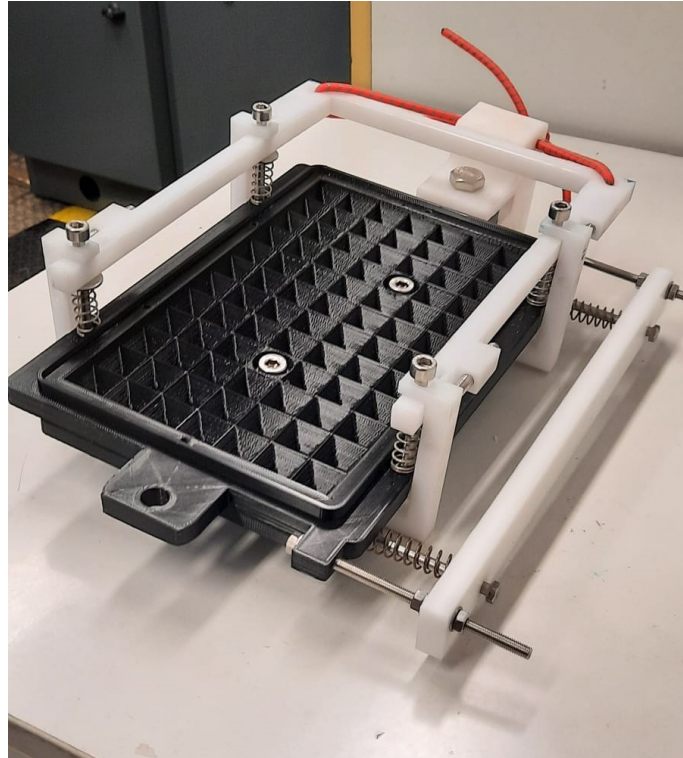


Figure 6.4: Manufactured LDM, fasten the elastic rope (the red rope), and with the activator (on the right) and the trigger, equipped with all springs and screws and one spout component

6.5 Dimensioning the spring force

With the chosen trigger, spring force sizing is an essential part of the LDM designing process. Most of the required movement is caused by springs. The calculation can be seen as a theoretical test of whether the mechanism will work.

6.5.1 Elastic force calculation for the springs

In order to calculate the exact force needed to move the mechanism, two calculations must be made. First, the force applied by the elastic springs from the trigger. Six springs can be used to apply the force, the four springs under the frame and the additional two springs placed on the guide screws. The formula for calculating the force that one spring can create can be seen in formula 6.1.

$$F_s = \Delta x \cdot D [22] \quad (6.1)$$

Where D is the spring constant, which is specific to each spring, and Δx is the length between the relaxed and the compressed spring.

Various compression springs made of the corrosion-resistant material Hastelloy were used based on their availability and suitable length.

All used springs were purchased from the company Gutekunst Co.KG. To apply pressure to the LDM, the springs are compressed by the mechanism by 20 mm. The spring constant can be taken from their website as $D = 1,59 \text{ N/mm}$. The result is a spring force of 31,8 N per spring at maximal compression. [23]

As seen in chapter 6, four springs are used around the frame. In addition, integrated into the grids, the same spring is screwed onto the two guide screws in order to make the

pressure applied by the screws calculable. The lower springs are compressed over a length of 10 mm.

This creates a parallel arrangement. Parallel arrangements of springs are calculated with:

$$F = \sum_{i=1}^n F_i [22] \quad (6.2)$$

Overall the applied force equals 159 N.

6.5.2 Friction coefficient calculation

$$F_F = \mu \cdot F_t > F_s \quad (6.3)$$

The frictional force (F_F) can be calculated from the coefficient of friction (μ) which depends on the material of the components. It also depends on the lubricating material, which in this study is salt water. The weight of the upper grid can be neglected, as it is significantly less than the spring force (weight of the upper grid: 0.472 kg), especially as the weight in water will be even smaller.

From the literature, a dependence between the friction coefficient and the printing temperature has been determined. At a printing temperature of 205 °C, the friction coefficient of PLA is given with $\mu \sim 0.27$ [24]. As the mechanism will be used in saltwater, saltwater plays a crucial role as a lubricant. However almost no data can be found on the topic, the calculation is made for a dry test first.

$$159N \cdot 0.27 = 42.9 \text{ N}$$

With relaxed springs the friction force is $44.5 \text{ N} \cdot 0.27 = 12.0 \text{ N}$ since the relaxed springs are still compressed by two millimeters.

Based on this result, the lateral spring force has to be greater than 13.3 N and less than 42.9 N. For the lateral movement, different springs are used, with a spring constant of $D = 0.497 \text{ N/mm}$.

With $12.0 \text{ N} / (2 \cdot 0.497 \frac{\text{N}}{\text{mm}}) = 12.1 \text{ mm}$, assuming that two springs are used for lateral movement, the compressed length is 12.1 mm at minimum. More springs can be used if necessary for a changed friction characteristics in the water.

As the range of movement is limited by the guide screws, only a 9 mm path for the grid is possible. It was therefore decided to use 13 mm as an end length for the compressed lateral springs so that the overall force is larger.

Practical tests confirm the calculation.

An elastic rope is planned for the movement of the blocking frame. Since this force does not need to be precise, no calculation is made. The force must be high enough to pull the frame out, but there is no maximum, as the force is efficiently blocked.

Practical tests in both salt and fresh water indicate that water increases the coefficient of friction. The detailed modifications that have been made follow the same calculations, but with an estimated, higher coefficient of friction. This will be considered in chapter 7.

7. Results

As a final test, the LDM was deployed during the cruise HE616 in the North Sea in April 2023. This was meant to show, whether the functions worked as planned. However, previous to the final tests, the mechanism needed to be implemented and tested in a laboratory environment. This was necessary to make sure that the LDM is working according to its basic principle.

7.1 Implementing the LDM

During the implementation and assembly of the individual components, it was realized, that some of the theoretical designs could not be executed as planned. Non-functional details become occasionally only apparent during installation or in the test phase. Subsequently, the implementation of the components will be discussed. It will be explained which parts caused problems:

The connecting board could not be implemented, because it did not fit onto the frames of the lower grid. The printing was not precise enough. Eventually, the connecting board was omitted, since it was supposed to create a better friction coefficient, and PLA has a friction coefficient that is sufficiently low. The lower grid was printed again without the frames.

However, since the lower crossbars (LDM - 006) were designed with a certain length to fit the thickness of the upper grid, lower grid, and connection board, a component had to be added to the lower crossbars to compensate for the lack of material thickness of the omitted component.

The range of motion for the trigger frame (LDM - 005) was not large enough. The leading core screws for the springs were blocked in their movement by the elongated holes (as planned), but too early to pull the bolts out completely and allow the springs to decompress. As a solution the part where the thread is located was shortened, to allow the bolts to get pulled out completely.

Both the bolts and the core screws had to be turned smaller to avoid jamming. The stability of the lower crossbar components was low when the trigger frame was pulled out. Therefore, an additional component (sidewall) was added, that can be screwed onto both extensions of the lower crossbars. This connection increased the stability.

An easy application was part of the criteria. While the filling and the operations are indeed easy, the implementation is a little challenging.

The force of the elastic rope was difficult to be installed only with the sprout component, more stretch length is needed. It can be connected to the mounting.

Instead of one mechanical trigger, two had to be used because of the huge applied force by the elastic rope, it came to a misalignment otherwise.

7.2 Results from the tests in a laboratory environment

Multiple tests were performed with the assembled mechanism. Firstly, the mechanism was tested in the air. This also helped to estimate the stretching length of the elastic rope. After it was determined that the mechanism worked reliably in the air during several tests, it was tested in an aquarium with fresh water. In figure 7.1 the test is shown.

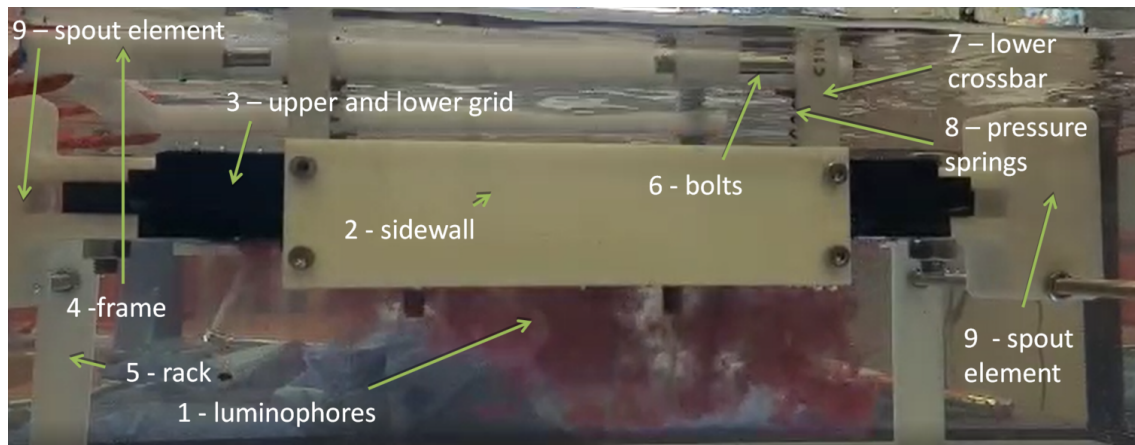


Figure 7.1: The LDM during the test in the aquarium

For a better understanding of the individual components, which are also mostly in the same colors, the figure will be explained with the help of the numbers. While the luminophores are coming out of the mechanism (1), the new sidewall (2) blocks the view. The sidewall connects the lower crossbars (7) to each other. The upper and the lower grids (3) are indistinguishable. A rack is added (5) to provide a stable distance to the floor. The spout components (9) are fastened. The one on the left is used to tension the elastic rope.

The trigger with the lower crossbars (7), the frame (4), which was pulled out by the elastic rope, the pressure springs (8), and the bolts (6) to keep the springs in the compressed position are visible.

The mechanism did fulfill its purpose and worked reliably during several tests. When force was applied to the red elastic rope, the frame was always pulled out. If the frame did no longer compress the springs, the activator triggered movement and the openings did always align.

However, two problems were noticed. After immersing the LDM in the water, air bubbles developed in the funnels of the lower grid. Due to the hopper form, they could not escape. The air bubbles prevented the luminophores from falling out, causing a high misalignment between different apertures, as the air bubbles collapse at different times. Admittedly, air bubbles will collapse due to pressure in deeper waters. Therefore, this is not expected to cause any problems during in-field use.

Secondly, the system appeared fragile. When confronted with external force, the grids opened partly. It will be observed if a partly opening of the grids will take place due to the movement through the water column and wave force during the HE616.

Additionally, the LDM was implemented into the SPI, as this is the setup for the final test. This was a test for the mounting, as well as for the mechanical trigger. The mechanical movement was simulated manually and the LDM was tested together with the SPI.

7.3 Experimental setup of the tests in the North Sea

The setup of the final test includes the LDM, which is mounted in front of the glass window of the SPI, with the described mounting from section 5.3. A technical description of the

SPI will be given.

First designed in 1984 by Drs. Joseph Germano and Donald Rhoads, the SPI are now used all around the world for many different campaigns. An example is the use as f-SPI by M. Solan in 2003. [4] [10]

The Sediment Profile Imaging Camera is a system that was designed for in situ imaging of the sediment-water interface. [25]

The SPI is a model 3731-D Remote Ecological Monitoring of The Seafloor (REMOTS) and is designed for in situ image analysis. A Nikon D7100 with a 24.1 megapixel Charged Coupled Device (CCD) array is used as a camera. The field of view is 216 mmx 152 mm, equaling the area of the plexiglass window. For optimal illumination, the flash power is six Watt seconds.[26]

A weight of 257 kg with an additional weight set of 113 kg in total in the air with only a few cavities allows the system to sink to the sea floor. The weight is also necessary to enable the prism to slam into the sediment to get an image of the layers. [26]

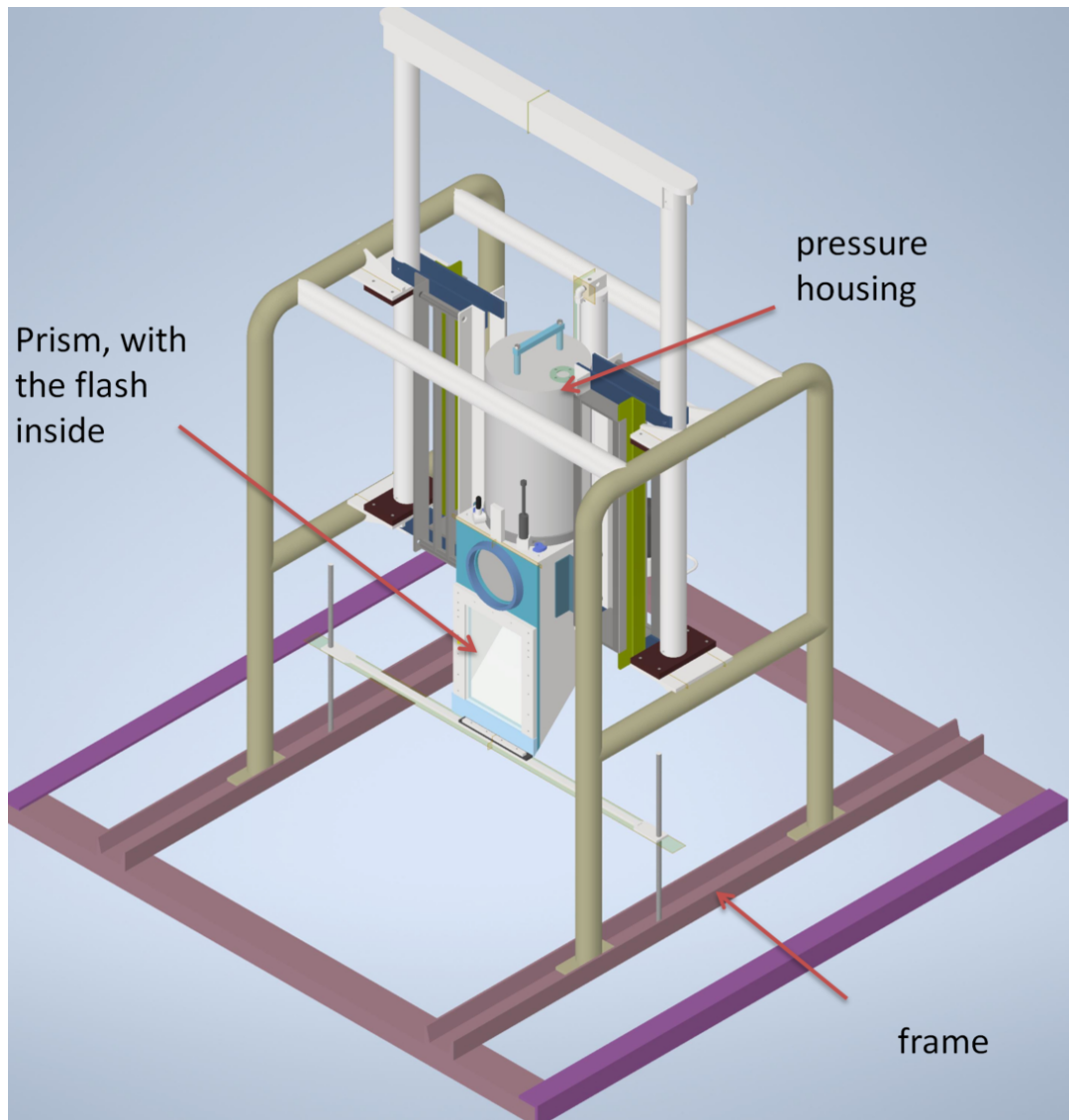


Figure 7.2: Sketch of the SPI Camera, drawn in Inventor

In figure 7.2 the SPI is presented with the prism, the pressure housing, the flash, and the

frame. The system also includes a trigger switch which cannot be seen in the figure. The prism is filled with distilled water or with alcohol in the case of a low-temperature surrounding, for instance, the polar deep sea to prevent freezing. It is located under the blue wall in figure 7.2. Inside, an inclined mirror allows the camera, mounted in the pressure housing right above, to see through the plexiglass window.

The pressure housing contains the camera, the electronic components, and the batteries. On the bottom, a glass pressure window is located, as well as a flash tube. All of the external components are made from stainless steel. [26]

The trigger switch is bolted to the main frame and is activated by the movement of the system. It is connected to the housing assembly by an underwater connector.

Important for the luminophore experiments is the flash tube. It is mounted inside a protective tube, which is attached to the pressure housing. Therefore, the flash tube itself is inside the prism. A plastic baffle, located above the mirror, eliminates light reflections. [26]

This whole system is implemented in a frame, which provides stability while lowering the system and taking pictures. Also, this adds weight to the system, and additional weight containers and attachment point fast to the prism in the middle.

The final test was conducted during the cruise HE616 with the *RV Heincke*. Following the example of previous tests, the SPI was placed into the ground and left there for about five hours to get a time series. In order to visualize bioturbation, luminophores have to be placed directly in front of the glass window of the SPI, which is done by the LDM. It is tested if the LDM spreads the luminophores evenly onto the seafloor, if a good visible result is possible, if the trigger and activator work as designed and if bioturbation is detected. Figure 7.3 shows the ready-to-use LDM during the cruise.

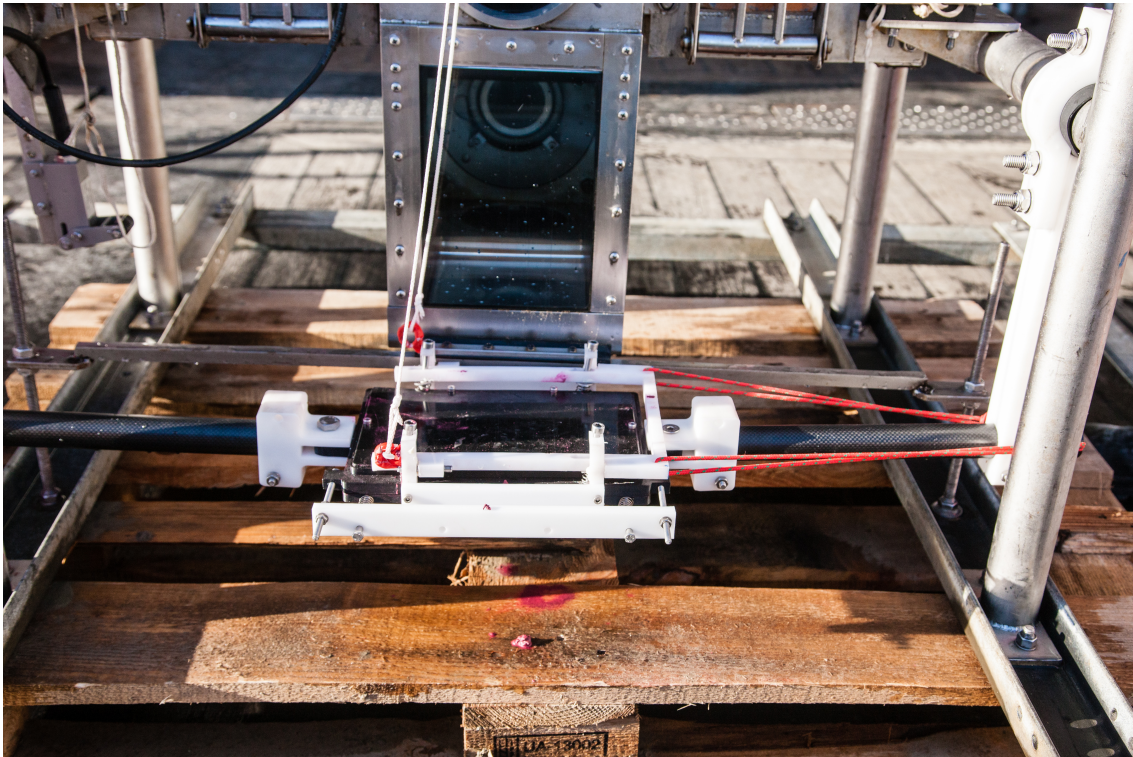


Figure 7.3: The LDM mounted in front of the SPI, on board of the *RV Heincke*, ready to be used

7.4 Results from the tests in the North Sea

However, problems occurred during the deployments. During the tests, the mechanical triggers were pulled out by the movable part of the SPI, but the frame was most often not extricated. The pressure on the grids was not released and therefore the mechanism did not open.

Even though only one test was planned, good weather, also seen in figure 7.4, conditions made it possible to carry out further tests. In total, five tests were conducted. For a better overview, the results are given in table 7.1.

Table 7.1: Details from the tests in the North Sea

Test number	1	2	3	4	5
Date	04.04.23	04.04.23	04.04.23	05.04.23	05.04.23
Time	8:00 - 13:00	15:00 - 16:00	16:40 - 17:00	09:00 - 09:20	09:40-10:00
Mechanical trigger	released	released	released	released	released
Release of the frame	no	no	3/4	yes	3/4
Opening of the grids	no	no	no	yes	no
Flushing rate of luminophores	0 %	0 %	0 %	20 %	0 %
What was changed	increase force	double force	lubrication, shorten springs	-	-

First, the two problems observed during the laboratory test can be evaluated. On the one hand, calm weather and sea conditions resulted in no wave force excitation of the system, which can be seen in figure 7.4. The movement through the water column did not cause an opening of the grids.

On the other hand, the air bubbles formed in the lower grid. The flushing out rate of the LDM was very low.

The changes that were made to improve the result are presented briefly in table 7.1. The increase in force refers to the force of the elastic rope on the frame. A higher force results in a higher chance of pulling out the frame. The bolts were lubricated with boat grease in the fourth and fifth attempts and the compression springs were shorted.

Due to the small dispersion rate of the luminophores (which can be seen in figure 7.5, the upper grid is still full of the pink luminophores), no image of the sediment layers with luminophores was taken.



Figure 7.4: Lowering the SPI into the water from the *RV Heincke*

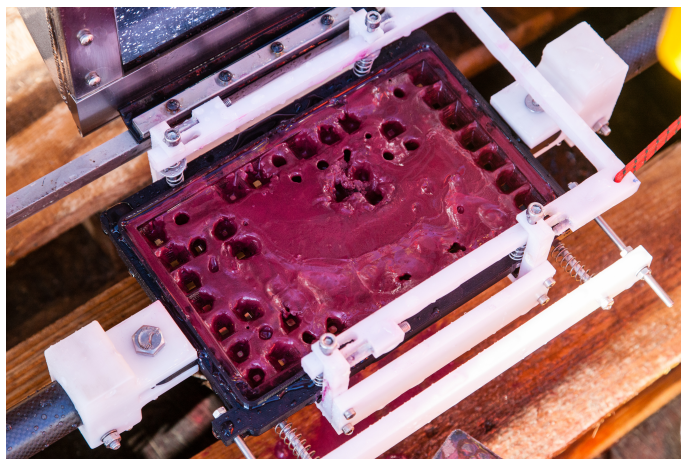


Figure 7.5: The LDM during the cruise with the *RV Heincke* after the fourth test

8. Discussion of the results

As various tests have been performed in different environments, the differences are clear: While the tests in the air as well as in laboratory environment can be seen as a success, the tests in the North Sea did not produce the desired result.

During the assembly, many components needed to be altered. First improvements were both necessary and successful, as could be seen during the tests in the air. The results of these tests show that the basic structure works and in addition, the spring forces for use in air have been calculated correctly.

It must be taken into account that the use of the LDM in water can change certain material properties. In particular, all points where friction occurs between the materials have a changed coefficient of friction due to the lubrication through the water.

Still, the result from the test in the water tank showed a successful deployment. It has to be mentioned, that the springs from the leading screws had to be left out in order to secure a reliable working of the mechanism. The lubrication through water seems to increase the friction coefficient between the two grids. With a lower overall applied force, the mechanism works as before.

The importance of an in-field test is stressed when reviewing the results from the North Sea. The results were extremely different from the tests in the air and freshwater. It has to be kept in mind, that many external influences change in comparison to previous tests. This includes a higher pressure, occurring currents, turbulence due to the penetration of the SPI into the seafloor as well as a different composition for the surrounding water. The water of the North Sea differs from the freshwater, which was used in the laboratory tests. Water in the North Sea has high salinity and consequently density. The temperature may vary, as well as in the water including organisms, sediment, and microplastics. All of this led to the different behavior of the LDM during the in-field test.

The main problems during the North Sea test can be taken from table 7.1 and include the release of the frame and the flushing out rate of the luminophores. Despite various improvements during the in-field tests such as lubricating the bolts and increasing the force from the elastic rope, the frame was only released one time. Additionally to that, the flushing out rate of the luminophores was really low. From observing the upper grid after the deployment (to be seen in figure 7.5), most of the luminophores stayed in the grid. Only the rows on the left and right sides appear empty.

The flushing out rate can be only evaluated from the fourth test in the North Sea, as this was the only one where the grids opened. When the grids did not open, no luminophores were washed out accordingly.

Possible improvements for the release of the trigger and the flushing out rate will be given. However, to find a solution for the problems during the North Sea test, the reason for failure has to be known.

Beginning with the trigger, possible reasons may have been an altered spring constant in the elastic rope due to soaking and therefore a different force. Additionally, the bolts might have been stuck in the holes of the lower crossbars due to increased friction with saltwater

as a lubricant. Organisms, sediment, or other suspended solids could have additionally increased the friction.

The flushing out rate might be decreased by several parameters. Air bubbles were observed during the laboratory test and will have formed during the North Sea test as well. However, they collapsed in the aquarium. That might not have been the case in the North Sea due to overfilling of the container.

The mechanism was never fully filled during the laboratory experiments due to the lack of available luminophores. It might be possible that a stuffed luminophore container might hinder air bubbles from climbing upward through the container, freeing the hopper.

Reasons, why the washed-out luminophores during test four were not visible with the f-SPI, might have additional reasons, such as strong currents or turbulence. The sinking behavior might have changed due to pressure.

Various improvements could be done to ensure a better result for the release of the frame. As lubrication of the bolts improved the result, lubrication is a recommended step for the future. Also, friction from the bolts could be further decreased by designing the bolts significantly smaller than the holes in the lower crossbars.

It was observed that during the 3/4 releases of the frame, only one bolt was not pulled out, while the other ones were free. This is only possible since the frame is too bendy. The frame should be revised and reinforced.

Also, the distance at which the frame is pulled out could be increased, for a more reliable result. The distance from the bolts to the frame is currently only two millimeters. The distance could be increased to six millimeters for instance. Additionally, the stretching length of the elastic rope should be increased, if possible.

Solutions for the flushing-out rate are a little more difficult. It is assumed, that this problem did mostly occur due to air bubbles in the grid. One solution would be to leave out the hoppers in the lower grid but rather install a flat surface.

Also, partrac advises using a mixing ratio of one kilogram of luminophores to six liters of water. This was not followed for this study, as a too liquid mixture resulted in water leaking out. Filling the container less dense might be a solution though. As the labyrinth seal allows water to flow in, the mixing ratio will alter itself once the mechanism is inside the water.

A different sealing for the lid of the container might be possible, allowing water to flow in and wash out the luminophores more easily. Individual tests should be performed to optimize the dispensing rate.

Opposed to the problems that occurred, the components that did work as designed in the North Sea have to be mentioned as well. The mechanical trigger was released during each test. It was found to work extremely reliably. Furthermore, the activator did open the grids when the frame was completely released. A higher force for the activator could result in an opening of the grids even though the frame is only 3/4 released. This might be a reasonable improvement for further deployments. Still, the activator did work as designed.

9. Conclusion

The goal of this bachelor's thesis was to develop a Luminophore Dispensing Mechanism (LDM) to be used in the deep sea with the fluorescent sediment profile imaging camera. Therefore, the main part was the development using different methods such as preliminary tests, evaluations based on criteria, and precise calculations.

Through preliminary tests, the method of using two movable grids was determined. This way, the change between the luminophore-containing state and the luminophore-dispensing state can easily be realized. A trigger to activate movement in the mechanism was included and evaluated, based on criteria. The main idea was to introduce movement with compression springs. The activator itself as well as the trigger, which prevents the grids from aligning, were realized that way. Through calculations based on the friction coefficient of the two moving grids, the necessary compression length of the springs was determined. However, the calculation was only precise for the use in air. Additionally, the expected lateral drift was calculated. On basis of the sinking behavior, which followed the equation of Stokes, a lateral drift was determined with 59 mm, for the worst case scenario.

Finally, practical tests were realized in a laboratory environment and in the North Sea. Though the LDM worked fine in the laboratory, luminophores were not dispensed in the North Sea.

Based on the knowledge of the previous experiments, goals for the LDM were formulated in the introduction. Among others, this included a uniform distribution of the luminophores. This criterion was not fully met. A uniform distribution of the luminophores could not be determined as a result, especially in the North Sea. In the laboratory, the uniform distribution was insufficiently tested. This criterion was therefore not fulfilled.

In contrast, however, the LDM is cost-efficient and has a short execution time. The automatic triggering is successful regarding the mechanical trigger and does not include direct human input. Furthermore, large water depths are no problem for the LDM and the test has a high repeatability, so it can be executed exactly the same several times.

The relatively short preparation time of the LDM for deployment, as well as the automatic triggering underwater, make the mechanism a device that is relevant for the future. For the implementation of time series with the SPI, the LDM is an indispensable addition for the future, as it saves time and effort and is cost-efficient. Thus, no further work step has to be performed after the SPI has been set down on the seafloor. Despite the fact that the distribution of the luminophores does not work reliably at the moment, the device is promising for the future if the basic idea is further developed. Corresponding suggestions for improvement were given in chapter 8, such as reinforcing the frame and performing further tests for the flushing-out rate.

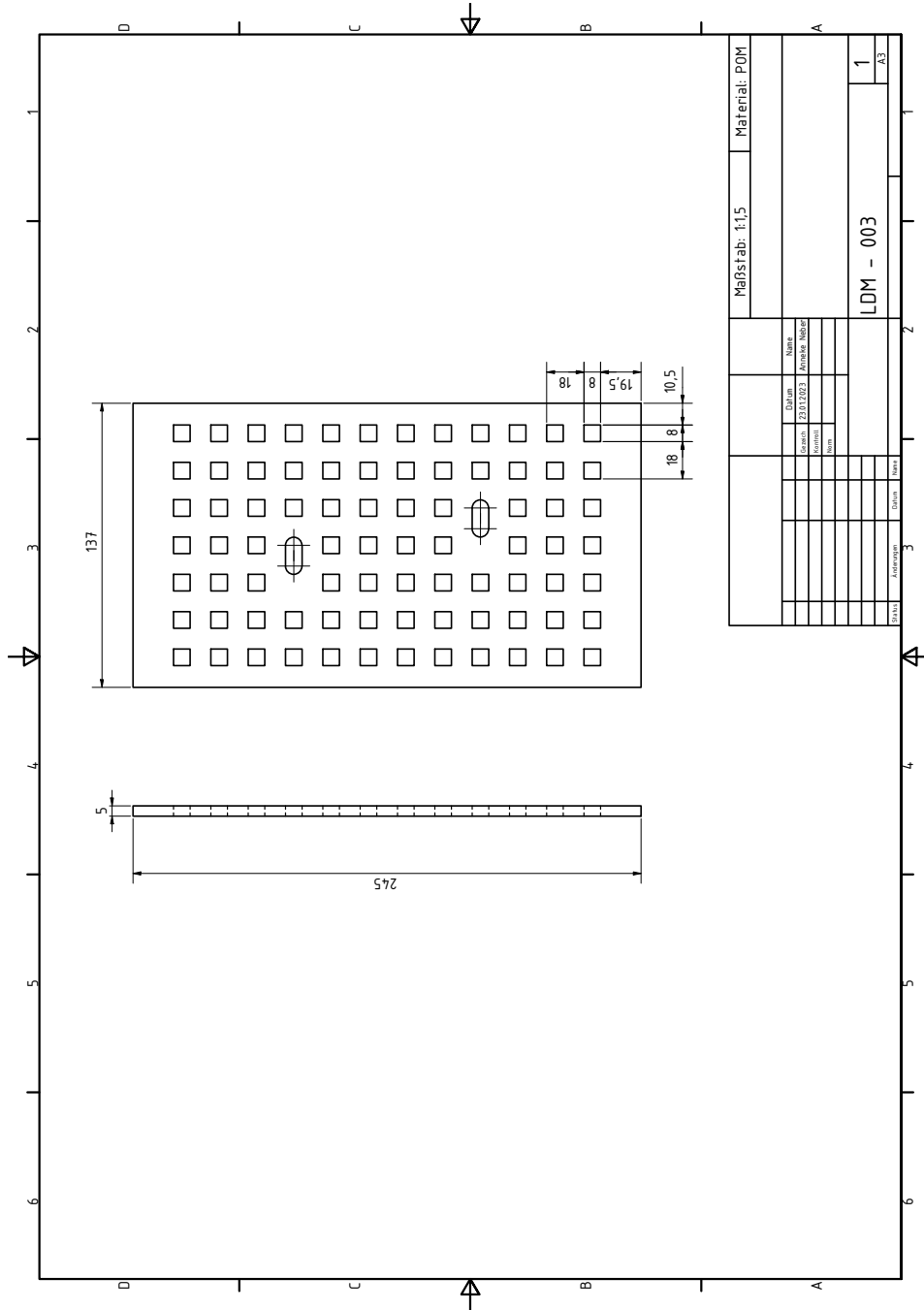
Based on the current prototype and mentioned improvements Luminophore Dispensing Mechanism will be further developed, so that it can be used during the expedition to the Arctic deep sea in 2024. Therefore, the development can be considered a success.

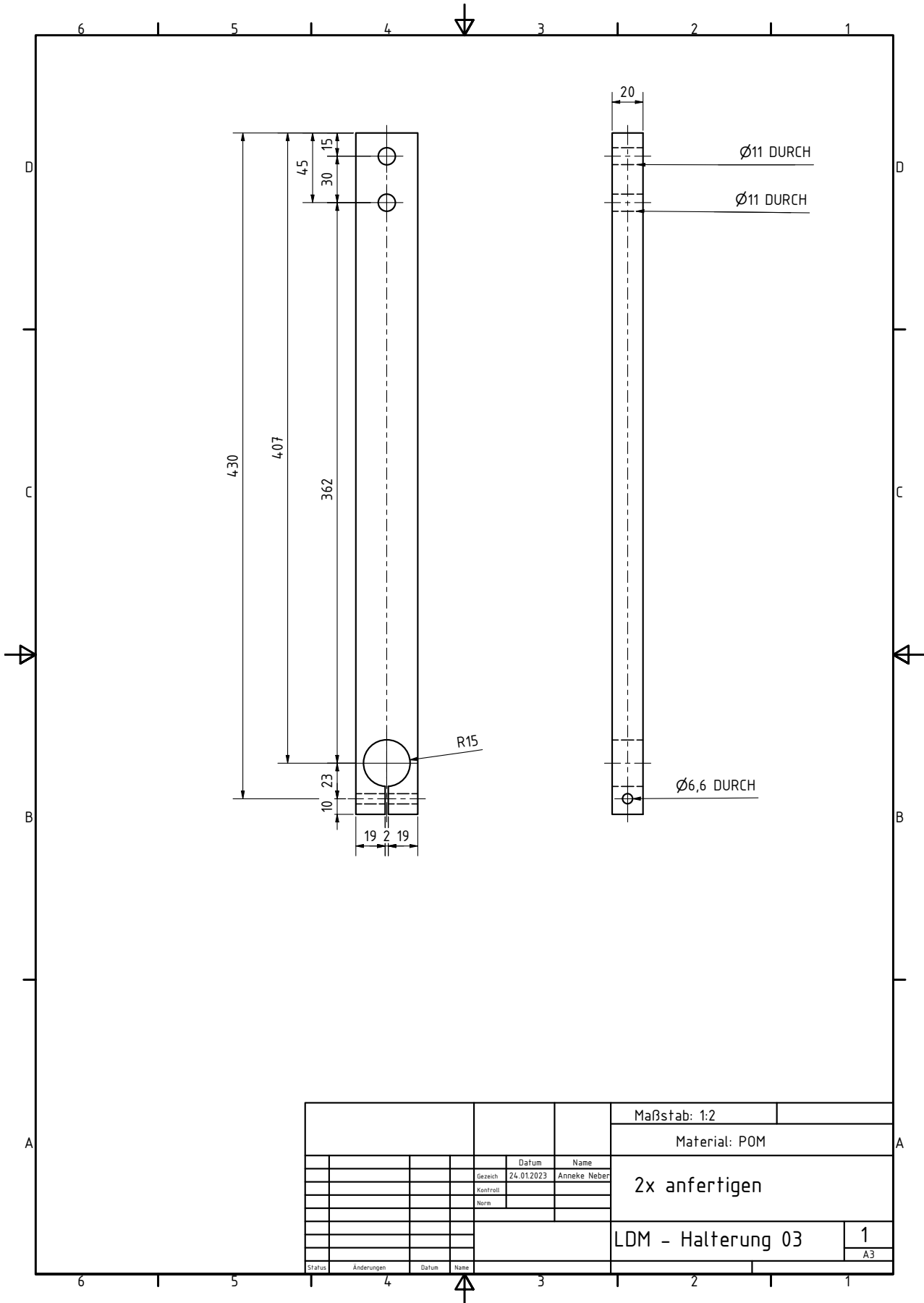
10. Bibliography

- [1] Martin Solan et al. “Climate-driven benthic invertebrate activity and biogeochemical functioning across the Barents Sea polar front”. In: *Philosophical transactions of the royal society a mathematical, physical and engineering sciences* 378 (2020). DOI: <https://royalsocietypublishing.org/doi/10.1098/rsta.2019.0365>.
- [2] Thomas Soltwedel et al. “Bioturbation rates in the deep Fram Strait: Results from in situ experiments at the arctic LTER observatory HAUSGARTEN”. In: *Journal of Experimental Marine Biology and Ecology* 511 (2019), pp. 1–9. DOI: <https://www.sciencedirect.com/science/article/pii/S002209811730686X>.
- [3] Spektrum. *Bioturbation*. <https://www.spektrum.de/lexikon/geowissenschaften/bioturbation/1876>. Accessed on 06.02.2023.
- [4] Martin Solan et al. “In situ quantification of bioturbation using time-lapse fluorescent sediment profile imaging (f-SPI), luminophore tracers and model simulation”. In: *MARINE ECOLOGY PROGRESS SERIES* 271 (2004). DOI: <https://www.int-res.com/articles/meps2004/271/m271p001.pdf>.
- [5] Christiane Hasemann et al. “Effects of dropstone-induced habitat heterogeneity on Arctic deep-sea benthos with special reference to nematode communities”. In: *Marine Biology Reserach* 9 (2012). DOI: <https://dx.doi.org/10.1080/17451000.2012.739694>.
- [6] Kevin Black. *Using Sediment Tracers to Map Sediment Transport Pathways*. http://csm.partrac.com/assets/files/using_sediment_tracers_to_map_sediment_transport_pathways_-_a_primer_kblack_final.pdf. 2012.
- [7] partrac. *partrac*. <https://www.partrac.com/>. Accessed on 08.02.2023.
- [8] *Lumineszens, Fluoreszens und Phosphoreszens*. <https://learnattack.de/schuelerlexikon/physik/lumineszenz-fluoreszenz-und-phosphoreszenz>. Accessed on 23.12.2023.
- [9] Eugene Hecht. *Optik*. Oldenbourg Verlag, 1999, p. 583.
- [10] Ocean Imaging Systems. *Model 3731-D REMOTS Digital Sediment Profiling Camera*. <http://www.oceanimagingystems.com/docs/REMOTS-3731D-24MP.pdf>. Accessed on 12.01.2023.
- [11] LEEdirect. *LEEdirect*. <https://leefiltersdirect.com/products/lee-filters-swatch-book-designers-edition-including-numeric-lookup?variant=32169227124830>. Accessed on 23.03.2023.
- [12] Ludwig Prandtl, Klaus Oswatitsch, and Kalr Wieghardt. *Führer durch die Strömungslehre*. Friedr. Vieweg Sohn, 1984, p. 173. ISBN: 3-528-18209-5.
- [13] Herbert Oertel jr. *Prandtl - Führer durch die Strömungslehre*. Springer Vieweg, 2016. ISBN: 978-658-08626-8.
- [14] Vladislav Gladkikh and Robert Tenzer. “A Mathematical model of the Global Ocean Saltwater density distribution”. In: *Pure and applied geophysics* 169 (2011). DOI: <https://doi.org/10.1242/jeb.220830>.

- [15] Abigail S. Tyrell, Houshuo Jiang, and Nicholas Fiscer. “Copepod feeding strategy determines response to seawater viscosity: videography study of two clanoid copepod species”. In: *Journal of experimental biology* 223 (2020). DOI: <https://doi.org/10.1242/jeb.220830>.
- [16] H. Schlichting and K. Gersten. *Grenzschicht-Theorie*. Springer, 2005, p. 30. ISBN: 3-540-23004-1.
- [17] Autodesk. *Inventor: Leistungsstarke Software für die mechanische Konstruktion für Ihre anspruchsvollsten Ideen*. <https://www.autodesk.de/products/inventor/overview?term=1-YEAR&tab=subscription>. Accessed on 27.01.2023.
- [18] Löwen Kunststoffe. *POM (Polyacetal)*. <https://www.loewen-kunststoffe.de/files/content/Downloads/Datenblatt~POM.pdf>. Accessed on 24.03.2023.
- [19] Larry E. Bird, Alana Sherman, and John Ryan. “Development of an Active, Large Volume, Discrete Seawater Sampler for Autonomous Underwater Vehicles”. In: *OCEANS 2007* 978-0933957-35-0 (2007). DOI: 10.1109/OCEANS.2007.4449303.
- [20] International Fishing Devices Inc. *Galvanic Time Releases*. <https://www.underseareleases.com/>. Accessed on 13.02.2023.
- [21] J.M. Paul, A.J. Paul, and Al Kimker. “Test of galvanic release for escape devices in crab pots”. In: *Regional Information Report 2A93-02* (1993). DOI: <https://www.adfg.alaska.gov/FedAidPDFs/RIR.2A.1993.02.pdf>.
- [22] Prof. Dr.-Ing. Günter Deiler. *Methodisches und beanspruchungsgerechtes Konstruieren, Vorlesungsbegleitendes Skript zum Studienmodul Konstruktionslehre Band 1*. 2018.
- [23] Gutekunst. *Gutekunst Federn*. <https://www.federnshop.com/de/>. Accessed on 14.02.2023.
- [24] Doina Frunuaverde et al. “The Influence of the Printing Temperature and the Filament Color on the Dimensional Accuracy, Tensile Strength, and Friction Performance of FFF-Printed PLA Specimens”. In: *Polymers* 14 (2022). DOI: <https://doi.org/10.3390/polym14101978>.
- [25] *Ocean Imaging Systems*. <https://oceanimagingystems.com/about.php>. Accessed on 12.01.2023.
- [26] Ocean Imaging Systems. *Instructions for the operation and maintenance of the ocean imaging system model 3731-D 4,000 meter digital sediment profiling camera*. 2018.

A. Technical drawings





		Maßstab: 1:2	
		Material: POM	
		2x anfertigen	
		LDM - Halterung 03	
		1	
		A3	
Status	Änderungen	Datum	Name

	Datum	Name
Gezeichnet	24.01.2023	Anneke Neber
Kontrolliert		
Norm		

B. Data sheets and other



Head Office: **Quotation No:** Q1243v02
 48 St Andrews Square **Project No:** P1000.02
 Glasgow **Date:** 09 Mar 2011
 G1 5PP **Created By:** JM
 UK
 Tel: +44 (0)141 552 3903

QUOTATION

Thomas Soltwedel
 HGF-MPG Joint Group for Deep-Sea Ecology and Technolog
 Alfred Wegener Institute for Polar and Marine Research
 27515 Bremerhaven
 Denmark

Cust Ref: 12/60068180 / 07.03.2011

Qty (kgs)	Description	Unit Price	TOTAL
2x 10	Silt sized tracer Density 2650 kg m-3, 60 um, fluorescent, paramagnetic. Pink.	£ [REDACTED]	£ [REDACTED]
10	Sand sized tracer Density 2650 kg m-3, 80 to 250 um, fluorescent, paramagnetic. Green.	£ [REDACTED]	£ [REDACTED]
Notes: Delivery time is approx 4 weeks.			
		Subtotal	£ [REDACTED]
		Shipping	£ [REDACTED]
		VAT 20.0%	£ [REDACTED]
		TOTAL	£ [REDACTED]